https://doi.org/10.5194/egusphere-2026-1203
Preprint. Discussion started: 9 April 2026

Elucidating the interplay between catchment and in-stream processes using high frequency multivariate and multisite data

Kenneth Gutiérrez-García[1, 2], Gunnar Lischeid[1, 2], Michael Rode[3]

[1] Leibniz Centre for Agricultural Landscape Research (ZALF), Müncheberg, Germany
[2] Institute of Environmental Sciences and Geography, University of Potsdam, Potsdam, Germany
[3] Department Aquatic Ecosystem Analysis, Helmholtz Centre for Environmental Research-UFZ, Magdeburg, Germany

E-mail address: kenneth.gutierrez-garcia@zalf.de (K. Gutiérrez-García)

Abstract. Stream water quality data provide essential insights into catchment biogeochemical processes. Continuous high-resolution measurements offer significant potential to differentiate between catchment-scale inputs and in-stream biogeochemical processing. Nevertheless, extracting clear, meaningful information from complex, multivariate time series spanning multiple variables and locations poses significant challenges. Using Principal Component Analysis (PCA) on high-resolution multivariate water quality data, this study aims to (1) separate catchment-scale contributions from in-stream biogeochemical processes, and (2) evaluate the dominant environmental drivers of spatial and temporal variability. The data were collected at five monitoring stations located in the Bode River, Germany. At each station, six variables were measured at 15-minute intervals over a period of seven years (2013-2020). The first principal component (PC1) accounted for 46% of the variance, capturing the typical seasonal impacts of stormflow dynamics. The second principal component (PC2) revealed the influence of saline groundwater upwelling, particularly during lowflow periods at specific sites. Diurnal fluctuations in pH, driven primarily by algal photosynthetic activity, were identified by the third component (PC3). Additional components highlighted localized processes: PC4, PC5, and PC6 were linked to turbidity variability during discharge peaks, while PC7 reflected anthropogenic influences, notably treated acid mine drainage entering the river. Lastly, PC8 described distinct nitrate dynamics observed at downstream monitoring sites. The application of PCA to high-resolution multivariate data proved to be very helpful in disentangling various catchment and within-stream effects on stream water quality. These findings emphasize the importance of advanced analytical techniques in unravelling complex hydrobiogeochemical dynamics.

1 Introduction

Water quality in rivers is a key indicator of both aquatic ecosystem health and human well-being. Continuous monitoring not only helps to quantify the presence of contaminants or variations in physicochemical parameters but also facilitates the anticipation and mitigation of environmental and public health risks (Chapman and Sullivan, 2022; United Nations Environment Programme, 2008). In this context, the use of high-frequency data is particularly valuable, as it allows the detection of subtle dynamics on daily, weekly, or even seasonal timescales (Lehr and Lischeid, 2020; Rode et al., 2016; Zink

https://doi.org/10.5194/egusphere-2026-1203
Preprint. Discussion started: 9 April 2026

et al., 2017. Such fluctuations, often overlooked when measurements are taken at lower temporal resolutions, can provide a more detailed understanding of the processes occurring within a watershed.

However, analysing extensive and complex time series poses significant challenges in hydrology, primarily due to the complicated stochastic characteristics inherent in hydrological data (Di et al., 2014). Numerous process-based studies have revealed complex, nonlinear interactions among different transport and turnover processes (Lischeid et al., 2017). As large volumes of information from multiple monitoring stations accumulate, distinguishing short-, medium-, and long-term patterns and isolating the key factors driving observed water quality variability becomes increasingly difficult. This complexity can hinder watershed modelling, given the necessity to describe water and mass fluxes, as well as the transformation processes occurring in various compartments, such as soil, vadose, and saturated zones, including surface and groundwater interactions (Rode et al., 2010).

Consequently, advanced statistical and computational methods are essential to enable integrated analyses that account for simultaneous interactions among multiple variables. Multivariate techniques capable of reducing dimensionality while preserving dominant temporal and spatial signatures are particularly critical to disentangle overlapping hydrological processes (Gewers et al., 2018; Jolliffe and Cadima, 2016). Among these, Principal Component Analysis (PCA) has emerged as a robust tool for addressing such challenges. Originally developed to identify orthogonal modes of variability in high-dimensional datasets, PCA has been widely adopted in environmental sciences. Initially applied in meteorology and oceanography to analyse spatial and temporal patterns in physical systems (Preisendorfer and Mobley, 1988), its utility has expanded to hydrological studies, where it aids in deciphering non-stationary signals, isolating dominant drivers of water quality variation, and differentiating catchment-scale processes from in-stream dynamics (Diamantini et al., 2018; Kröcher et al., 2025; Lehr and Lischeid, 2020; Meggiorin et al., 2022; Yue et al., 2020). Its ability to reduce dimensionality while preserving critical patterns makes it particularly suited for untangling overlapping processes in heterogeneous datasets.

This study aims explicitly at extracting information from the short-term temporal patterns of various water quality parameters. We assume that a small number of effects prevails affecting all or most of the observables, although varying in severity between parameters and sampling sites. Then PCA application to a high-resolution multivariate, multi-site dataset can be used as a diagnostic tool to decompose and separate concurrent environmental processes operating at different scales. Therefore, this study uses PCA to (1) discriminate between watershed-scale contributions and in-river biogeochemical processes that determine water quality and (2) identify the main environmental drivers responsible for spatial and temporal patterns in multivariate water quality data.

2 Study area

The study area is the Bode catchment (Fig. 1), located in northern Germany. It includes part of the Harz Mountains and extends towards the Magdeburger Börde area in the East. This catchment has been intensively monitored by the TERrestrial ENvironmental Observatories network (TERENO, Wollschläger et al., 2017), operated by the Helmholtz Centre for

https://doi.org/10.5194/egusphere-2026-1203
Preprint. Discussion started: 9 April 2026

Environmental Research-UFZ. In this study, data of five water quality stations of TERENO will be used, three of which are located in the Selke subcatchment: Silberhütte (SH), Meisdorf (MEI) and Hausneindorf (HAU). The remaining two stations are located in the lower part of the Bode catchment: Groß-Germersleben (GGL) and Staßfurt (STF) (Table 1).

Table 1. Characteristics of the five water quality monitoring sites in the Bode River catchment.

Site Acronym	Site Name	Catchment Area (km²)	Location & Geography	Dominant Land Use	Key Features / Specific Influences
SH	Silberhütte	105	Upstream site on the Selke River	Primarily forested	Directly impacted by the effluent from an acid mine drainage (AMD) treatment plant located 550m upstream
MEI	Meisdorf	184	Transition zone site on the Selke River	Highly forested	Influenced by upstream primary production from deciduous mountain forests.
HAU	Hausneindorf	456	Lowland site on the Selke River subcatchment	Mixed, with dominant agriculture and forest cover	Located 700m downstream of a wastewater treatment plant (WWTP).
GGL	Groß-Germersleben	2485	Lowland site on the main stem of the Bode River	High-yield agriculture on fertile lowland soils	Situated over a salt dome
STF	Staßfurt	3200	Downstream lowland site on the main stem of the Bode River	High-yield agriculture	Influenced by the salt dome geology

The entire Bode catchment has an area of approximately 3,200 km² and an altitude ranging from 50 m to 1,142 m above sea level (m.a.s.l.). The Selke subcatchment has an approximate area of 456 km² and an elevation range between 68 and 597

https://doi.org/10.5194/egusphere-2026-1203
Preprint. Discussion started: 9 April 2026

m.a.s.l. It is important to note that, despite the location of HAU within the Selke subcatchment, this station is situated in the lowlands, as is GGL and STF, while SH and MEI are located in the upstream region of the Selke River in the lower Harz Mountains.

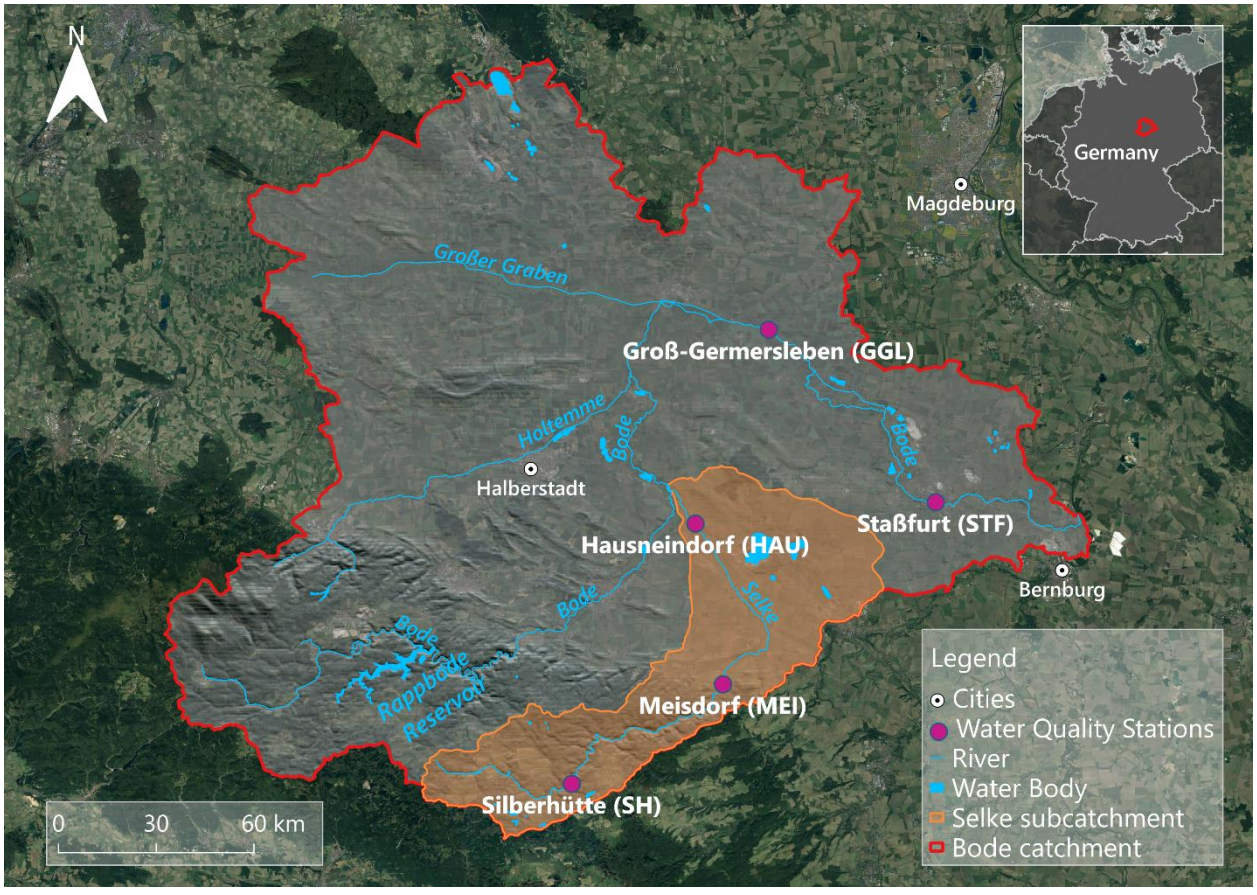

Figure 1. Map of the study region with the 5 sampling stations along the Selke and Bode River. Data source: Sampling stations and catchments by TERENO, Wollschläger et al., 2017; Water bodies and rivers by State Office for Surveying and Geoinformation of Saxony-Anhalt, 2025. Imagery © 2025 Image Landsat / Copernicus, Map data © 2025 Google Earth Pro, overlaid by a Digital Elevation Model (DEM) from Hartmann et al. (2023).

The geology of the Harz Mountains is predominantly composed of igneous and metamorphic rocks (Wollschläger et al., 2017). In this region, tectonic uplift, combined with the pronounced erosion of the former Mesozoic cover, has led to the formation of a prominent steep scarp along the northern Harz boundary (Diercks et al., 2021). In contrast, the lowland area is characterized by Mesozoic and late Paleozoic rocks, which are largely covered by Tertiary and Quaternary sediments (Wollschläger et al., 2017), resulting in thick porous aquifers. Due to a combination of density gradients and tectonic activity associated with the uplift of the mountain region, massive salt stocks and domes have formed in the lowlands, in some cases reaching the surface (Seibertz, 2020). Because of this, Staßfurt is widely known for its potash mining, which began in the 19th century (Kleine-Kleffmann, 2023; Luo et al., 2012)

https://doi.org/10.5194/egusphere-2026-1203
Preprint. Discussion started: 9 April 2026

The soils in the Harz Mountains are mostly relatively shallow, overlying fractured hard-rock aquifers. They primarily consist of Cambisols, with smaller proportions of Leptosols, Luvisols, and Gleysols (Wollschläger et al., 2017). In contrast, the lowlands are predominantly covered by Chernozems, which are known for their high organic matter content and fertility, making them well-suited for arable land use. Notably, the soils of the Magdeburger Börde are regarded as the most fertile soils in Germany, supporting high-yield agriculture and contributing significantly to the region's agricultural productivity (Altermann et al., 2005; Wollschläger et al., 2017).

According to Wollschläger et al. (2017), the CORINE 2006 (CORINE Land Cover, 2026) land cover map identifies that 26% of the basin's territory consists of forests and semi-natural areas, primarily located in the mountainous region. In contrast, around 66% of the lowlands is used for agriculture, while the remaining land cover, including cities, industrial areas, and both active and former open-pit mining sites, accounts for 7% of the basin. Water bodies and wetlands make up the final 1% of the basin, contributing to the region's biodiversity but occupying a relatively small portion of the landscape.

Meanwhile in the Selke subcatchment, land cover is distributed as follows: 48% agriculture, 40% forest, 6% urban areas, and 6% other uses. However, upstream of the SH station, the forest comprises 65% of the area, while between the SH and MEI station, the forest area corresponds to 75% (Winter et al., 2021). Further downstream towards HAU the land use is predominantly agriculture (48%), but still with an important part of forest (40%). There are six wastewater treatment plants (WWTPs) in the Selke subcatchment (Winter et al., 2021). But there are also more WWTP further downstream alongside the Bode River and its other tributaries. Among these, the WWTP located 700 m upstream the HAU gauge is of particular interest as it could have a direct effect on water quality. Additionally, there is an acid mine drainage treatment plant that discharges its water via a tributary into the Selke River 170 m upstream the SH station.

The significant elevation variation creates climatic differences. The mountains experience a cold, moist climate, whereas the Central German Lowland area is warmer and dryer (Schröter et al. 2005). This disparity is evident in precipitation patterns, with the upper Harz Mountains receiving over 1700 mm of annual precipitation, contrasting with the Central German Lowland plains, where annual precipitation falls below 500 mm. Additionally, mean annual air temperature varies significantly, ranging from approximately 5°C in the mountains to around 9.5°C in the eastern part of the Magdeburger Börde (Wollschläger et al., 2017).

The vulnerability of these regions to climate change has been assessed in various studies. According to a report by the German Federal Environmental Agency (Schröter et al. 2005), the Central German Lowland area, including the Bode catchment, is highly susceptible to climate change impacts, particularly due to low water availability, the increasing risk of summer droughts and the high risk of flooding (Wollschläger et al., 2017). Schröter et al. (2005) note that the cold and wet climate characteristics of these mountains made them less vulnerable to adverse events. However, in recent years, rising temperatures have led to droughts, which have weakened Norway spruce trees. Affected by this phenomenon, Norway spruce trees were infected by the eight-toothed spruce bark beetle (*Ips typographus*) starting 2018. It caused large dieback especially from 2020 on (Anders et al., 2025). This process could, increase surface runoff, soil erosion and nitrate leaching (Chen et al., 2024) but fully developed only after the end of the monitoring periods.

https://doi.org/10.5194/egusphere-2026-1203
Preprint. Discussion started: 9 April 2026

3 Materials and methods

3.1 Data sources

The data sets were provided by the Bode catchment hydrological observatory that is part of the TERENO network (Wollschläger et al., 2017; Zacharias et al., 2011; Zhang et al., 2023). This data set includes five stations (Fig. 1) measuring six variables: electrical conductivity, nitrates concentration (NO_3), turbidity, water discharge, water temperature, and pH. The data used here was collected at 15-minute intervals from November 2013 to December 2019. A complete summary of the descriptive statistics for each measured parameter at the five monitoring sites can be found in the Supplementary Material (Table S1). The dataset used in this study has an overall data coverage, averaging approximately 98% across all variables and sites for the seven-year period. Occasional gaps in the time series were filled using linear interpolation, implemented with the *na.interp()* function from the *forecast* package (Hyndman et al., 2023) in R.

Discharge increases substantially between HAU and GGL (Fig. 2) due to some major tributaries from the mountainous region (Fig. 1). In contrast, discharge differs only slightly between the SH, MEI and HAU sites and between the GGL and STF sites. The absence of a significant increase in discharge between MEI and HAU despite nearly doubling of the respective catchment area suggests low groundwater recharge in the lowlands, with most of the discharge being generated in the mountainous regions. This is consistent with a clear climatic gradient from the mountains to the lowland part of the catchment (Li et al., 2025).Correspondingly biogeochemical processes in the mountainous part of the catchment are likely to play a disproportionately large role.

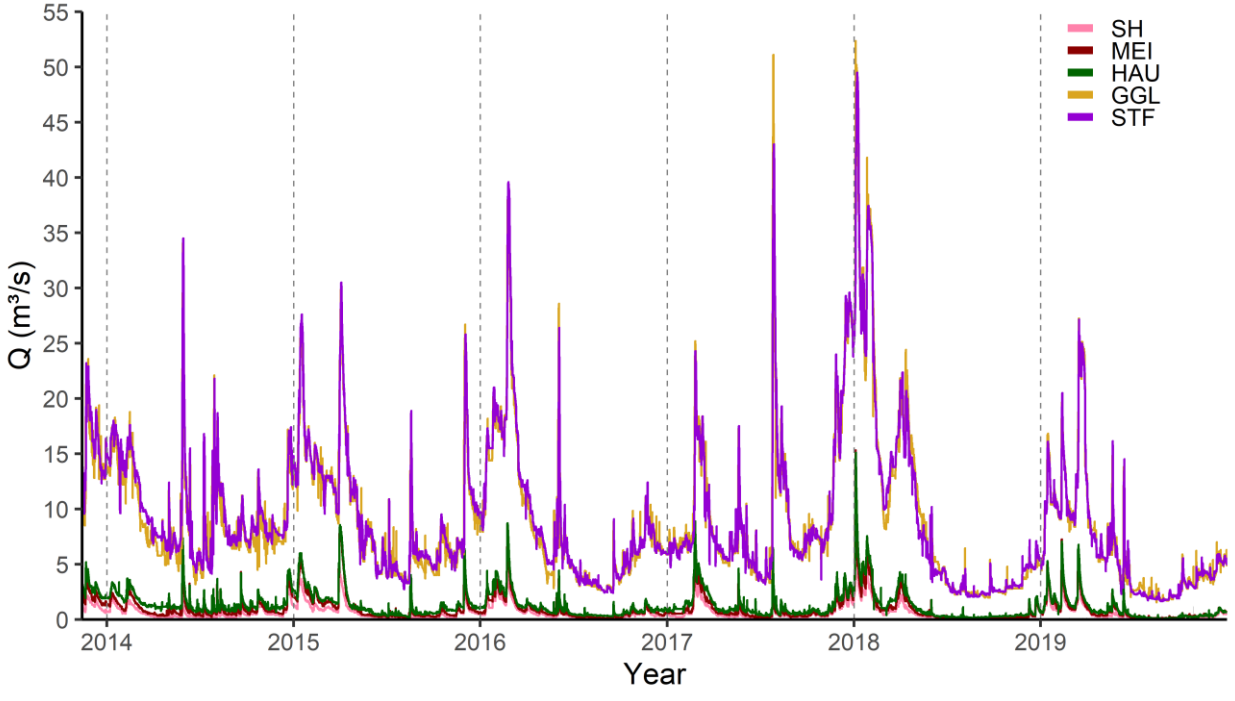

https://doi.org/10.5194/egusphere-2026-1203
Preprint. Discussion started: 9 April 2026

Figure 2. Time series of discharge at the five sampling sites.

3.2 Principal Components Analysis

Before performing Principal Component Analysis (PCA), exploratory data analysis was carried out to examine the cross-correlation structure between the measured variables. Spearman correlations were calculated for each site, and also separately by season of the year and by flow regime (low, medium, high). The resulting correlograms are presented in the Supplementary Material (Fig. S1, S2 and S3). This initial analysis provides essential context for the interpretation of the principal components. Principal Component Analysis (PCA) of time series, also referred to as Empirical Orthogonal Function (EOF) analysis, is widely used for dimensionality reduction and pattern recognition (Chen et al., 2015; Hannachi et al., 2007; Jolliffe, 1990). The term "EOF" is commonly used in climate and geophysical sciences, whereas "PCA" is more prevalent in statistics and machine learning. PCA serves as an orthogonal basis to decompose data variability where all principal components are uncorrelated, thereby facilitating signal analysis (Kim and Wu, 1999).

PCA is conducted by performing an eigenvalue decomposition of the covariance matrix of the time series. To ensure comparable contributions from all variables, data are typically standardized by subtracting the mean and dividing by the standard deviation (Preisendorfer and Mobley, 1988). Principal components are defined by the resulting eigenvalues and eigenvectors (Kim and Wu, 1999). The eigenvalues indicate the proportion of variance explained by each component. The number of principal components to retain is typically guided by criteria such as cumulative explained variance, with 80% to 90% of the total variance often considered sufficient. All analyses were conducted in R using the function *prcomp()* from the *stats* (R Core Team, 2023) package.

Based on the eigenvectors time series of scores are generated for each principal component, effectively capturing the dominant patterns of variability in the original dataset. The loadings, defined as the correlations between the original time series and the principal components identify the influence of each original variable on the components. This offers insights into their contributions to the observed patterns in the data.

Finally, the communality for each variable was calculated to assess how much of its variance is captured by the principal components. The communality of a variable is determined by summing the squared loadings of that variable across all the selected components. A high communality value indicates that the variance of a specific variable is well-represented by the selected components, whereas a low value suggests that a significant portion of its variance is unique and not explained by the components.

https://doi.org/10.5194/egusphere-2026-1203
Preprint. Discussion started: 9 April 2026

4 Results

4.1 Eigenvalues and variance

The first four principal components exhibited eigenvalues exceeding 1. They accounted for 71% of the total variance. Additionally, to the first four, four more were selected, thus having the first eight principal components corresponding in total with 84% of the variance. These components are described in more detail in the following sections.

Table 2. Percentage of variance explained, and cumulative variance for the first eight principal components of the PCA.

	Variance Explained (%)	Cumulative Variance (%)
PC1	46	46
PC2	13,2	59,2
PC3	6,4	65,6
PC4	5,5	71,1
PC5	4,2	75,3
PC6	3,1	78,4
PC7	2,9	81,3
PC8	2,8	84,1

Figure 3 shows the communality for each parameter and site, representing how much of the variance in each parameter is explained by specific principal components, color-coded from PC1 to PC8. Sampling sites are ordered from upstream (top) to downstream (bottom). Site Silberhütte (SH) is located in the mountain area, gauge Meisdorf (MEI) at the transition zone between mountains and lowlands, and the remaining sites further downstream in the lowlands (Fig. 1). These results provide insight into the main factors driving the variability of water quality across the catchment. For water temperature, discharge, nitrate, and electrical conductivity, variance is primarily explained by PC1 across all stations, indicating that this component captures the major influencing factors, likely related to climatic patterns and hydrological processes like precipitation and surface runoff, which affect the entire catchment uniformly. However, the variance of nitrate concentration at GGL and STF is mostly explained by a combination of PC1 and PC8, suggesting that these sites experience an additional unique local driver not present at upstream stations.

https://doi.org/10.5194/egusphere-2026-1203
Preprint. Discussion started: 9 April 2026

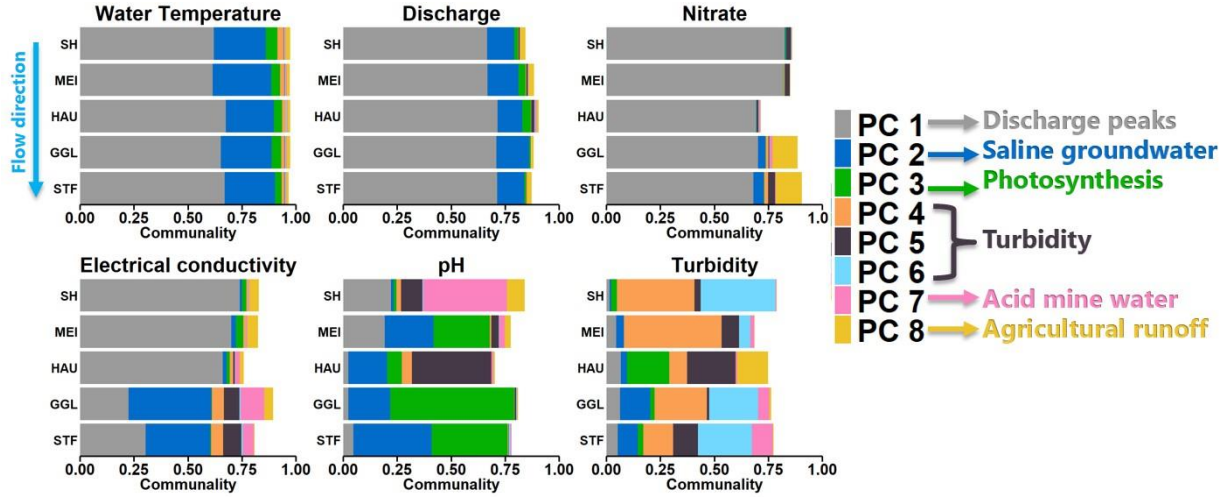

Figure 3. Communality of the different principal components (PCs) at different sites (SH, MEI, HAU, GGL, STF) and for different variables. Sampling sites are ordered from upstream (top) to downstream (bottom).

In the case of electrical conductivity, PC1 is dominant at the upstream stations, but not in the two lowstream stations (GGL and STF) where there is a major distribution of other components like PC2, PC4, PC5, and PC7, highlighting a more complex interplay of various processes. This holds even more for pH at all stations: At SH, PC1 and PC7 are the most important components, while at MEI, the first three PCs contribute roughly in equal parts. At HAU, pH is dominated by both PC1 and PC5. At GGL, PC3 prevails, while at STF, PC2 and PC3 have a similar contribution. Turbidity variance is distributed across multiple principal components. At the upstream sites SH and MEI, PC4 is dominant, and PC6 as well at SH. At the two downstream stations GGL and STF, variance is distributed across PC2, PC4, and PC6. At the mid-catchment station HAU, turbidity is mainly associated with PC3, PC5, and PC8.

4.2 First component

The first principal component accounts for 46% of the total variance in the data. The loadings of PC1 (Fig. 4) reveal consistent patterns across all stations: strong positive correlation with discharge and nitrate concentration, along with strong negative correlation with water temperature and electrical conductivity. In contrast, absolute values of the correlation coefficients for pH and turbidity are much smaller. For pH, there is a gradual increase, transitioning from moderately negative at upstream stations to positive at downstream stations.

An interesting pattern is observed for turbidity in PC1. For most sites, including the downstream GGL and STF stations, turbidity is negatively correlated with discharge. This suggests a large-scale dilution effect. The headwaters of the Bode catchment are heavily forested and regulated by a large reservoir system (Rappbode Reservoir), which acts as a massive sediment trap. During highflow events, the large volume of very low-turbidity water released from these upstream areas likely overwhelms the local sediment inputs from agricultural lands in the lowlands, resulting in a net dilution.

https://doi.org/10.5194/egusphere-2026-1203
Preprint. Discussion started: 9 April 2026

The contrasting positive correlation at the HAU site is a notable exception. HAU is located on the Selke River, a tributary not directly regulated by the large reservoir system. Here, the local signal is strong enough to dominate. The surrounding area is dominated by agricultural land use, and surface runoff from these fields during storms appears to contribute a significant sediment load, creating a positive discharge-turbidity relationship that is masked by large-scale dilution at the main river sites.

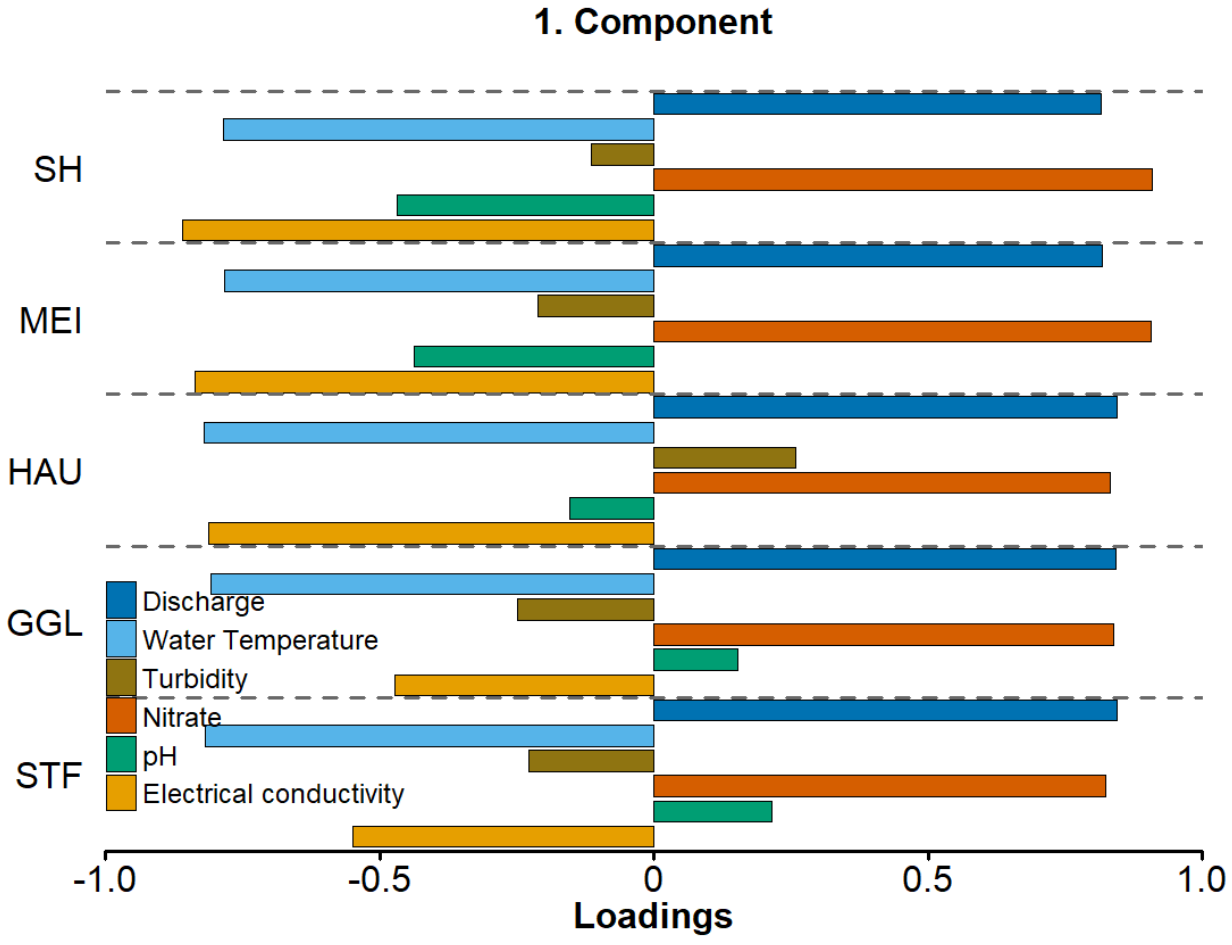

Figure 4. Loadings of the first principal component (PC1) on water quality variables across the five sampling sites (SH, MEI, HAU, GGL, STF), arranged from the upper (SH) to the lower (STF) parts of the catchment.

The loadings on PC1 reveal several key patterns. First, the consistently high positive correlation with discharge at all locations points to an effect that is closely related to discharge peaks. Secondly, the correlation with temperature reflects the seasonal variability of runoff, with higher discharge during colder periods. Thirdly, the positive correlation with nitrate at all locations, regardless of differences in land use, soil types or vegetation cover, suggests widespread topsoil pollution throughout the basin being mobilized during discharge peaks, involving both agricultural and forestry-dominated areas. Finally, the systematic change in pH loads reveals contrasting soil characteristics. In upstream areas, the topsoil is more acidic due to the low buffering

https://doi.org/10.5194/egusphere-2026-1203
Preprint. Discussion started: 9 April 2026

capacity of bedrock and soils. In contrast, in the downstream areas, the surface soil layers are less acidic than the deeper layers, reflecting the effects of the high intensity of fertilization and liming on farmland.

4.3 Second component

The second component (Fig. 5) shows a strong inverse relationship with discharge, water temperature, and turbidity across all sites. In the upper parts of the catchment, the negative correlation of turbidity with this component is weaker, whereas in the lower catchment areas, this correlation becomes more pronounced. In contrast, pH, nitrate and electrical conductivity display positive correlations at all stations although varying in strength depending on the site. At station SH, located in the upper catchment, the correlations are generally weaker than at downstream stations. Interestingly, at MEI and HAU (mid catchment), nitrate shows a lower correlation, which contrasts with the pH variable, where the correlation is much stronger. Meanwhile, correlation with electrical conductivity remains relatively consistent across the three upstream sites.

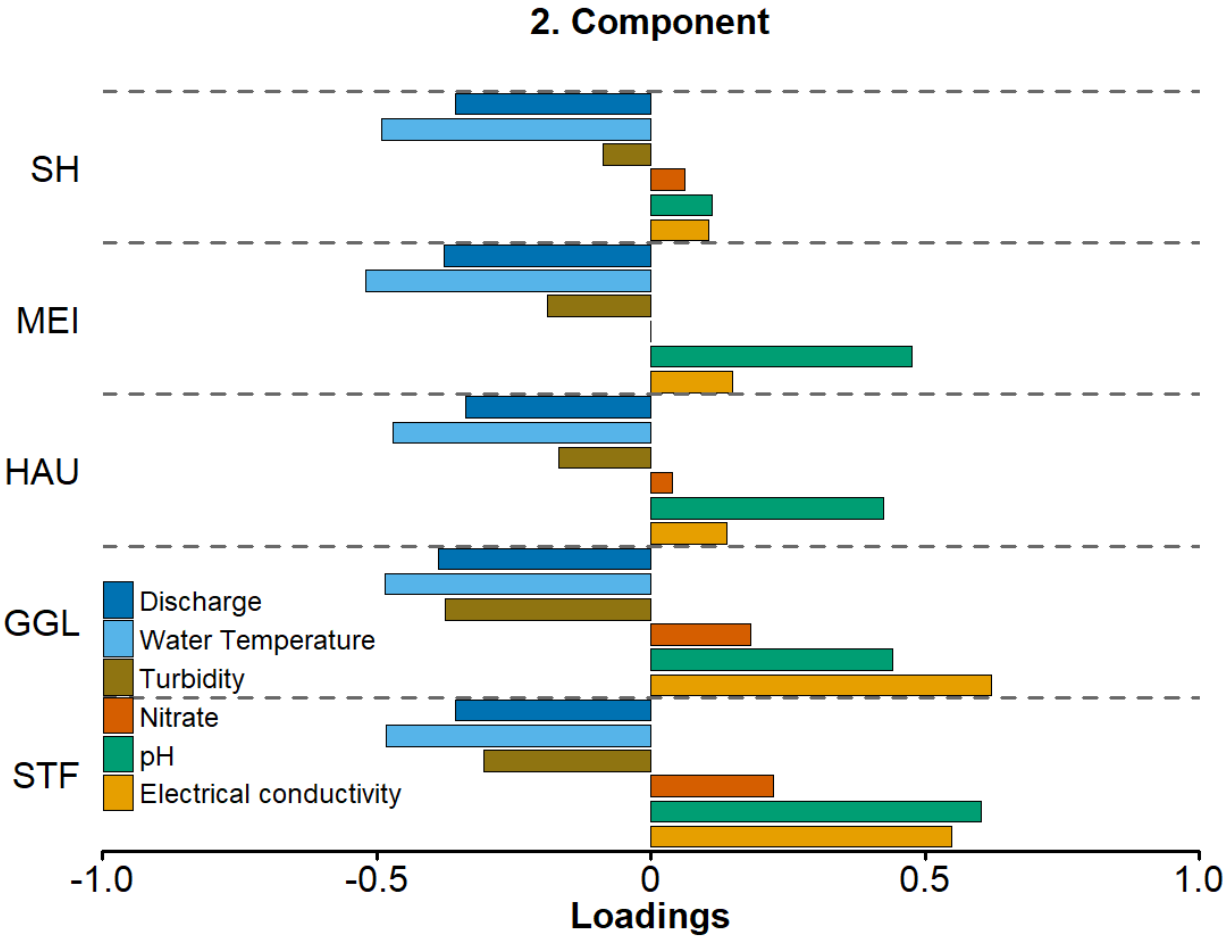

Figure 5. Loadings on the second principal component (PC2) for water quality variables across the five sampling sites.

https://doi.org/10.5194/egusphere-2026-1203
Preprint. Discussion started: 9 April 2026

The second principal component (PC2) captures the influence of groundwater on stream chemistry, characterized by periods of lowflow and high electrical conductivity. This contrasts directly with the storm flow dynamics represented by PC1. This inverse relationship is visually demonstrated in Figure 6, which shows that during periods of low discharge, PC2 scores are consistently high. Conversely, each major discharge peak corresponds to a sharp and immediate drop in the PC2 scores, highlighting the diluting effect of stormflow on the saline groundwater signal. However, in contrast to PC1 there are substantial differences between the upstream and downstream sampling sites.

The strongest positive loads for electrical conductivity are notably observed at the downstream stations GGL and STF. This is a direct reflection of local geology, as these two stations are located above a salt dome known to be connected to the river system. During periods of reduced river flow, groundwater contributes a greater proportion of the river discharge. Under these conditions, saline groundwater from greater depth can rise and enter the river, significantly raising salinity levels. This upwelling process, clearly isolated by PC2, highlights the fundamental role of geological controls in shaping water quality dynamics, especially during base flow.

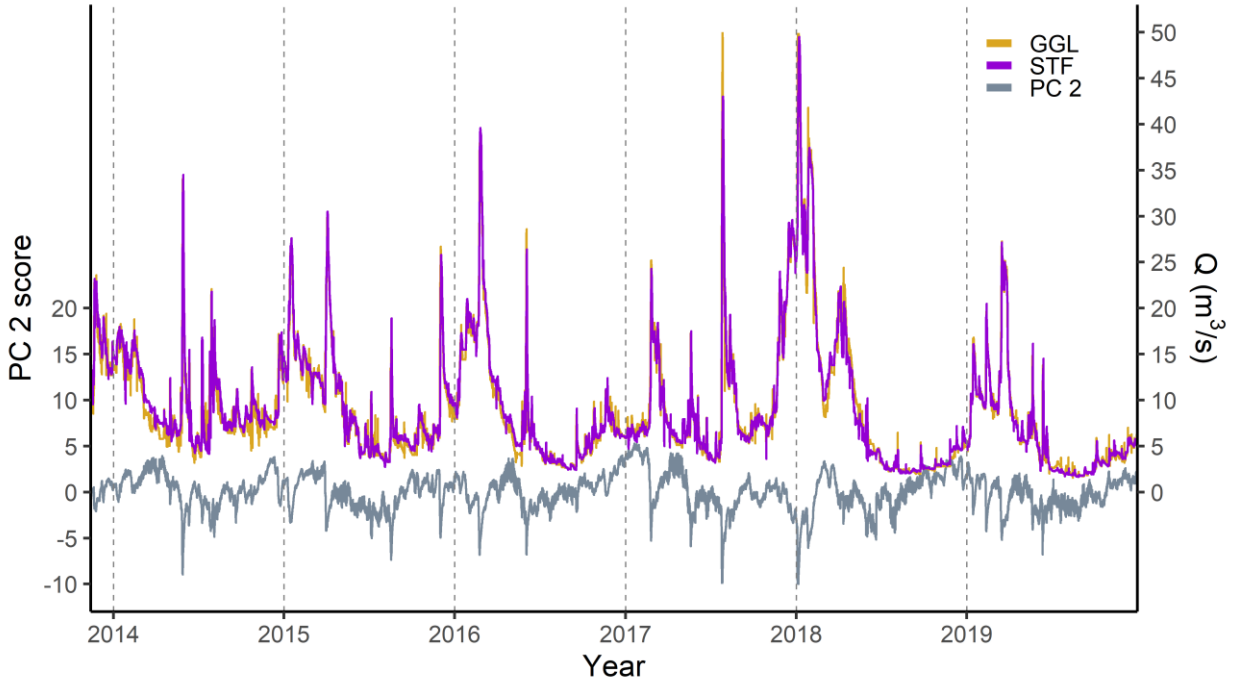

Figure 6. Comparison between discharge at GGL and STF and PC2 scores.

4.4 Third component

The third principal component (Fig. 7) shows weak correlation with most variables, except for notable correlation with pH at specific stations. Correlation with turbidity, while less pronounced, displays some spatial variability, particularly at HAU, where turbidity has its highest positive correlation, contrasting with weaker correlation elsewhere. At MEI, GGL, and STF, pH exhibits strong positive loadings, indicating its central role in this component.

https://doi.org/10.5194/egusphere-2026-1203
Preprint. Discussion started: 9 April 2026

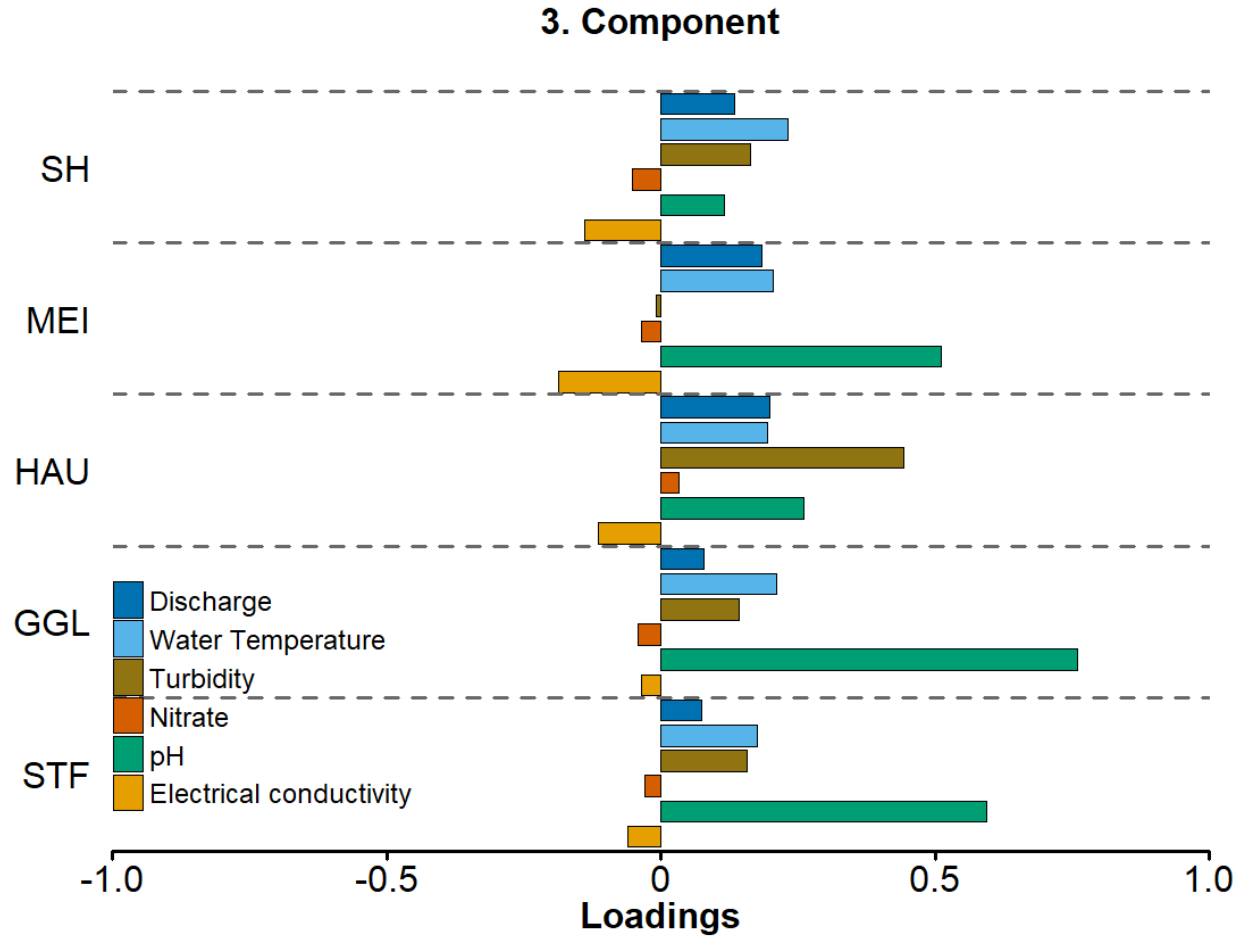

Figure 7. Loadings of the third principal component (PC3) for water quality variables across five sampling sites.

As illustrated in Figure 2, PC3 becomes increasingly relevant for explaining variations in pH at the downstream stations GGL and STF. This pattern suggests a growing importance of pH in the lower catchment, likely being linked to biogeochemical processes that vary spatially along the river's course. A closer look at the daily time series for both pH and PC3 (Fig. 8) reveals a diurnal cycle: levels rise during the day and fall at night. Note that Fig*ure* 8 depicts a baseflow period, where the effect of stormflow peaks on pH can be ignored (see PC1 and PC2). This pattern is likely driven by photosynthetic activity in the river, where algae uptake CO_2 and bicarbonate during daylight hours, reducing acidity and raising pH. At night, photosynthesis ceases but respiration continues, leading to increased CO_2 levels and a corresponding pH decrease.

https://doi.org/10.5194/egusphere-2026-1203
Preprint. Discussion started: 9 April 2026

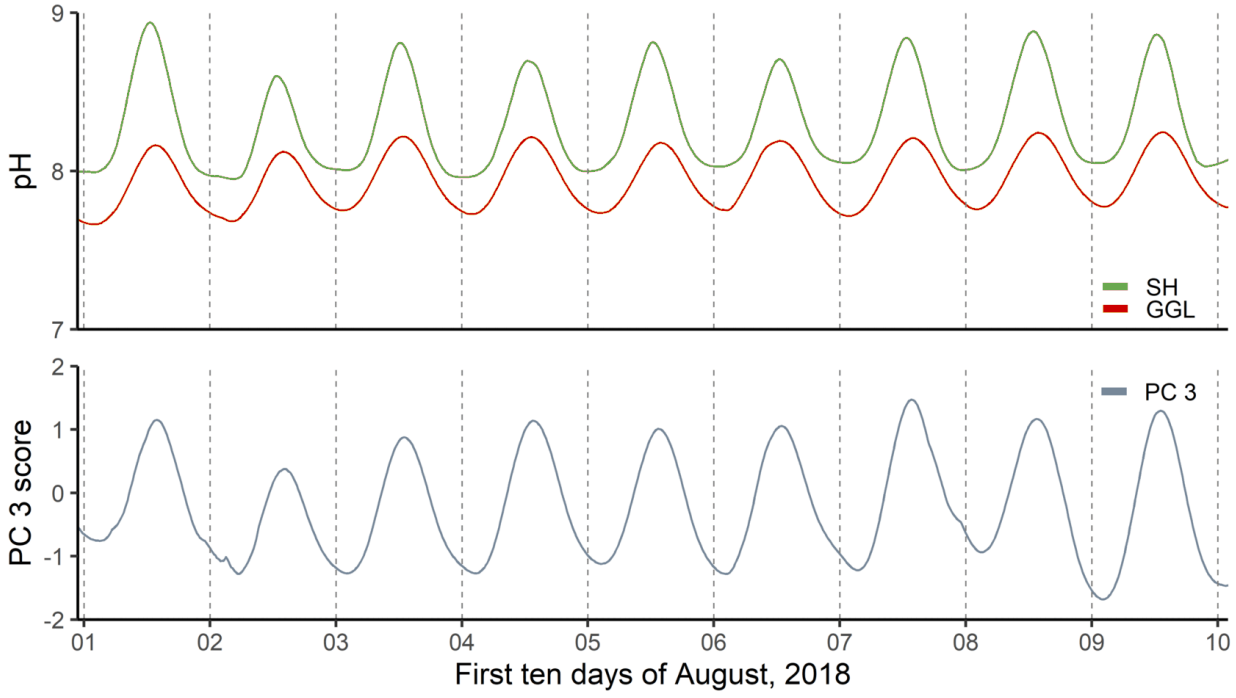

Figure 8. Comparison of pH time series for two sampling sites (SH and GGL) and the third principal component (PC3) during the first ten days of August 2018.

The strongest effects of PC3 are observed at the lowland sites GGL, STF, and the transitional site MEI. At MEI, the variability observed is influenced by upstream primary production originating from deciduous forested sites in the mountain range, which experience limited shading during spring. According to Rode et al. (2016), the length of the stream reach impacting MEI is restricted to approximately 3 km upstream. In the case of the GGL and STF stations this effect is likely due to the environmental conditions in these areas, where the wide valleys, lowflow velocity and the reduced shadowing by trees create an ideal environment in these regions that supports the proliferation of phytoplankton (Huang et al., 2022), phytobenthos or periphyton, thereby amplifying the influence of photosynthesis on the observed variability.

As the amplitude of diurnal fluctuation is traced back to photosynthetic activity it can be used as a proxy for daily photosynthetic activity as shown in Figure 9. Its time series shows a clear seasonal pattern, with higher amplitudes in the summer months and lower amplitudes in the winter. It also shows considerable variability across years. In particular, photosynthetic activity appears to have been more pronounced in 2018 and 2019, which were notably dry and warm years compared to previous years. Thus, the interannual variability in PC3 amplitude highlights the complex interplay between climatic factors and within-stream biological activity in shaping river water quality dynamics.

https://doi.org/10.5194/egusphere-2026-1203
Preprint. Discussion started: 9 April 2026

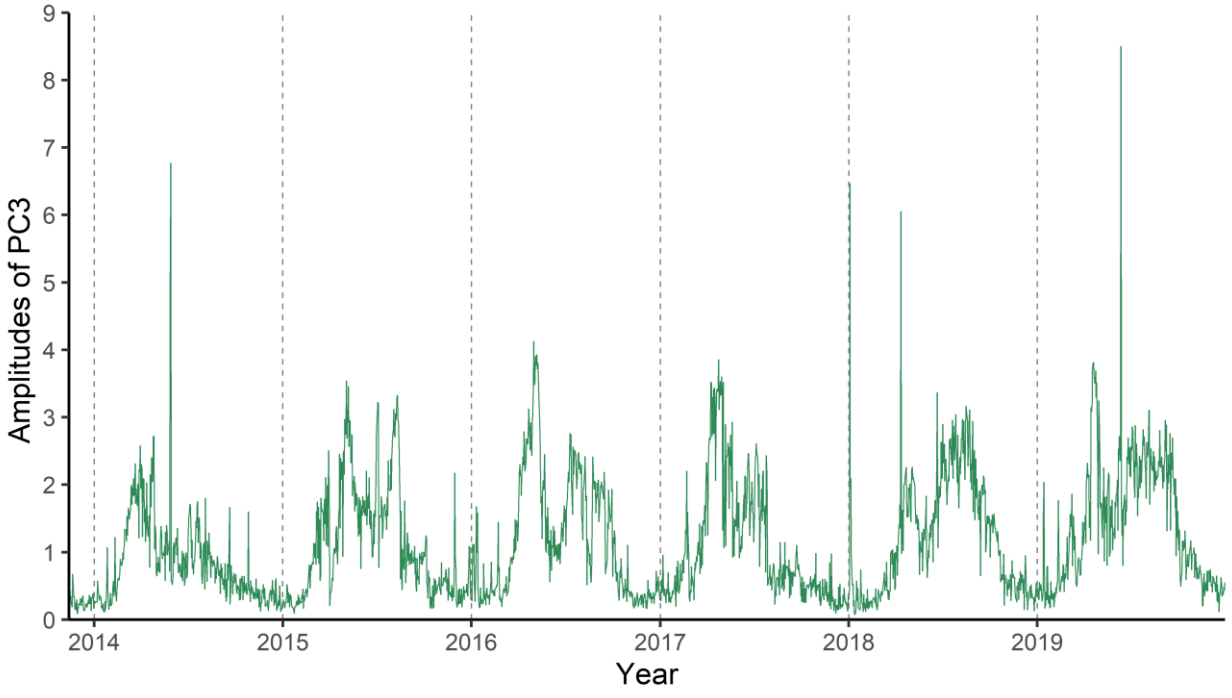

Figure 9. Time series of PC3 daily amplitudes from 2014 to 2019.

4.5 Fourth, Fifth and Sixth component

The fourth, fifth, and sixth principal components are highly significant as they collectively demonstrate the PCA's ability to deconstruct the complex behavior of a single parameter in this case turbidity. Rather than representing one uniform process, the analysis successfully isolates distinct turbidity dynamics that vary by site and event, as shown by their differing contributions in the communality plot (Fig. 3).

PC4, with its strong positive loadings across all sites (Fig. 10), appears to represent the general turbidity response to increased discharge common throughout the catchment. PC5 isolates a unique process at the HAU site, showing a strong negative correlation with turbidity (Fig. 11). Given HAU's location downstream of a WWTP, this suggests a localized dilution effect from the plant's effluent, a distinct signature that the PCA successfully discerned from the broader patterns. PC6 captures a spatial gradient in turbidity sources, with loadings transitioning from negative upstream to positive downstream (Fig. 12), likely reflecting a shift in dominant erosion processes along the river continuum.

By construction principal components are not intercorrelated. However, these components have in common that they exhibit either positive or negative peaks during discharge peaks. Thus, ignoring the differing signs by using the absolute values of the component scores only yields pairwise correlation coefficients between $r = 0.34$ and $r = 0.67$ (Fig. 13). That implies that these components grasp processes that play a role during discharge peaks mostly but differ between sites and between events. Note that every principal component explains part of the variance that has not already been explained by preceding components.

https://doi.org/10.5194/egusphere-2026-1203
Preprint. Discussion started: 9 April 2026

290 Thus, component four, five and six presumably reflect site- and event-specific processes as bank erosion, surface runoff, road drainage or even efflux from a wastewater treatment plant.

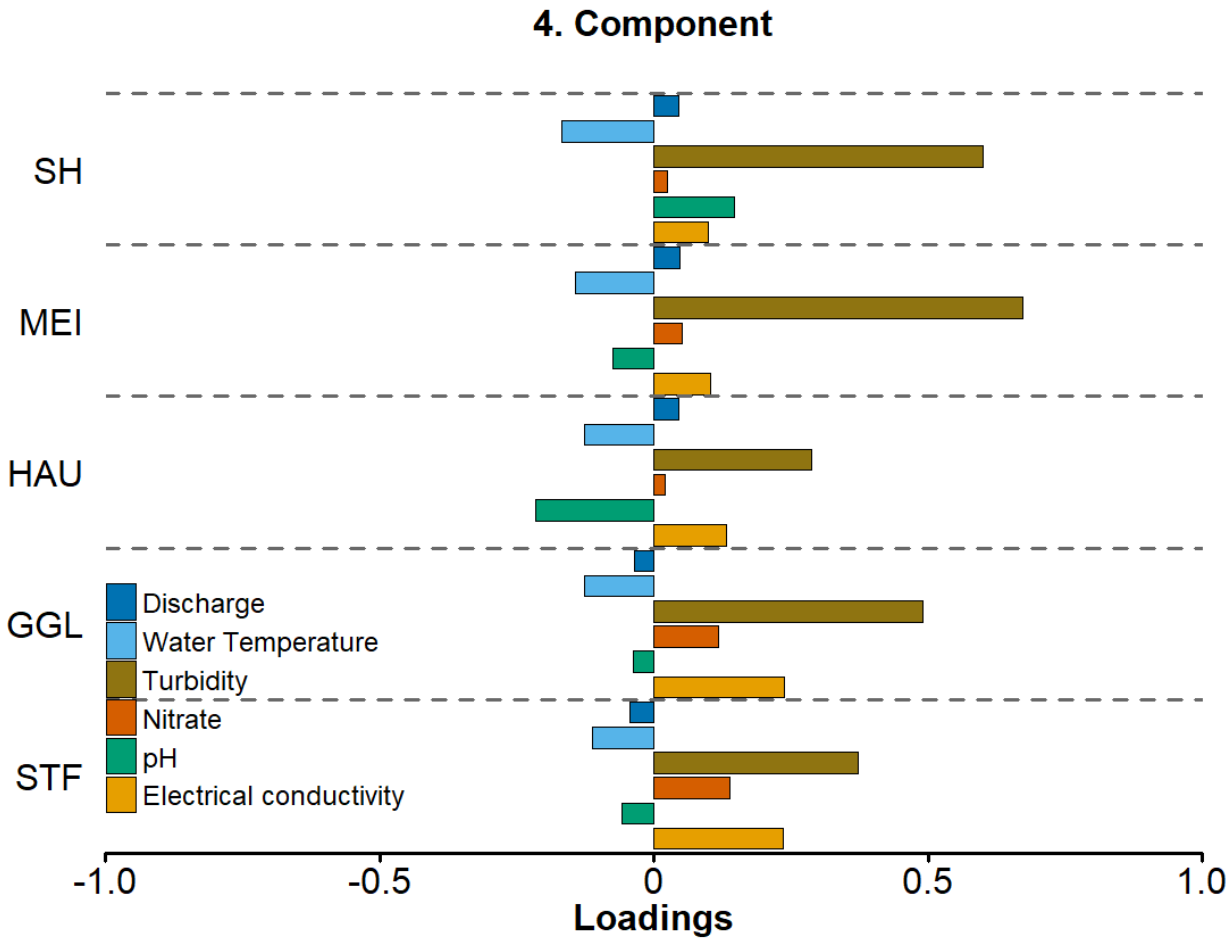

Figure 10. Loadings on the fourth principal component (PC4) for water quality variables across five sampling sites.

https://doi.org/10.5194/egusphere-2026-1203
Preprint. Discussion started: 9 April 2026

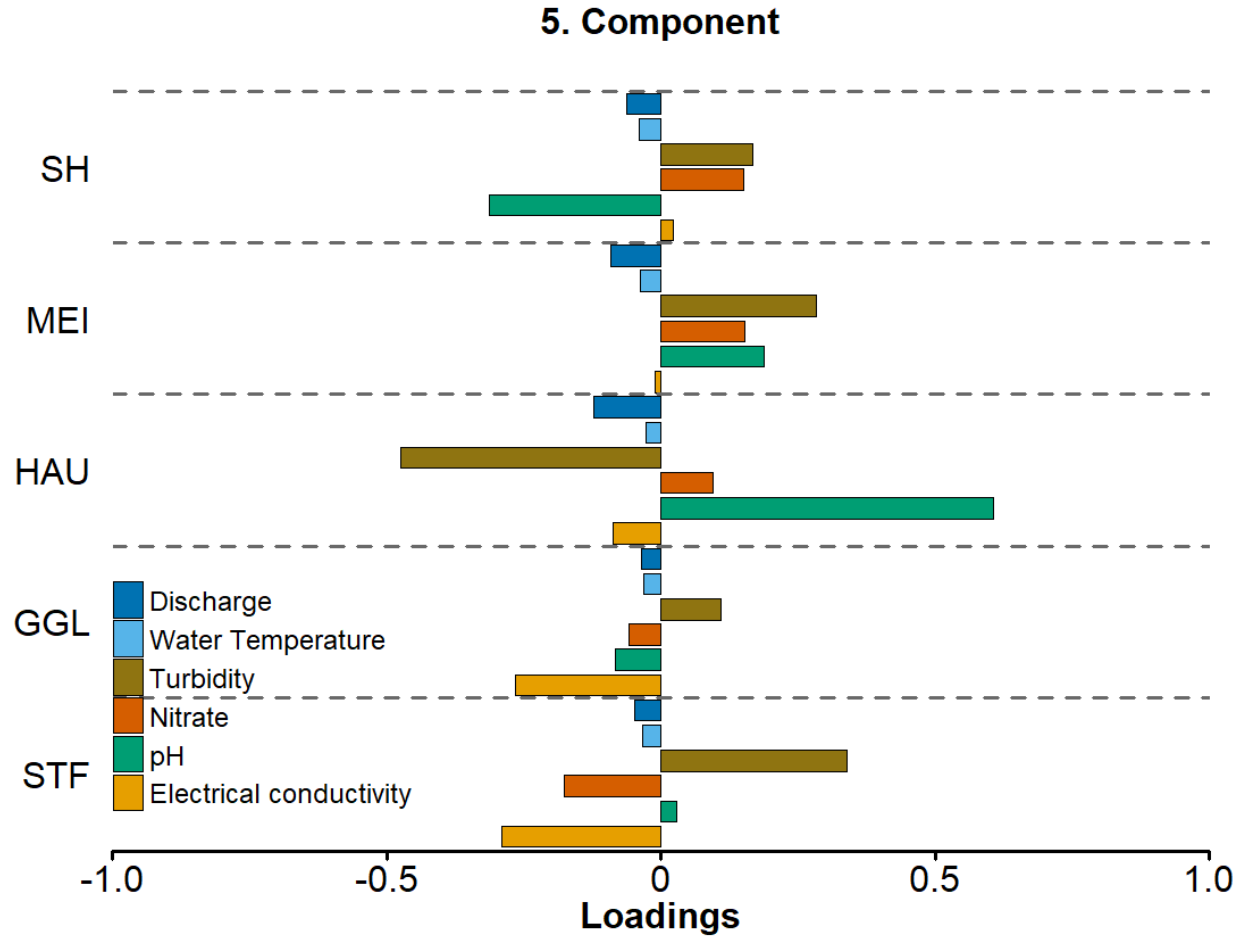

295 **Figure 11. Loadings on the fifth principal component (PC5) for water quality variables across five sampling sites.**

https://doi.org/10.5194/egusphere-2026-1203
Preprint. Discussion started: 9 April 2026

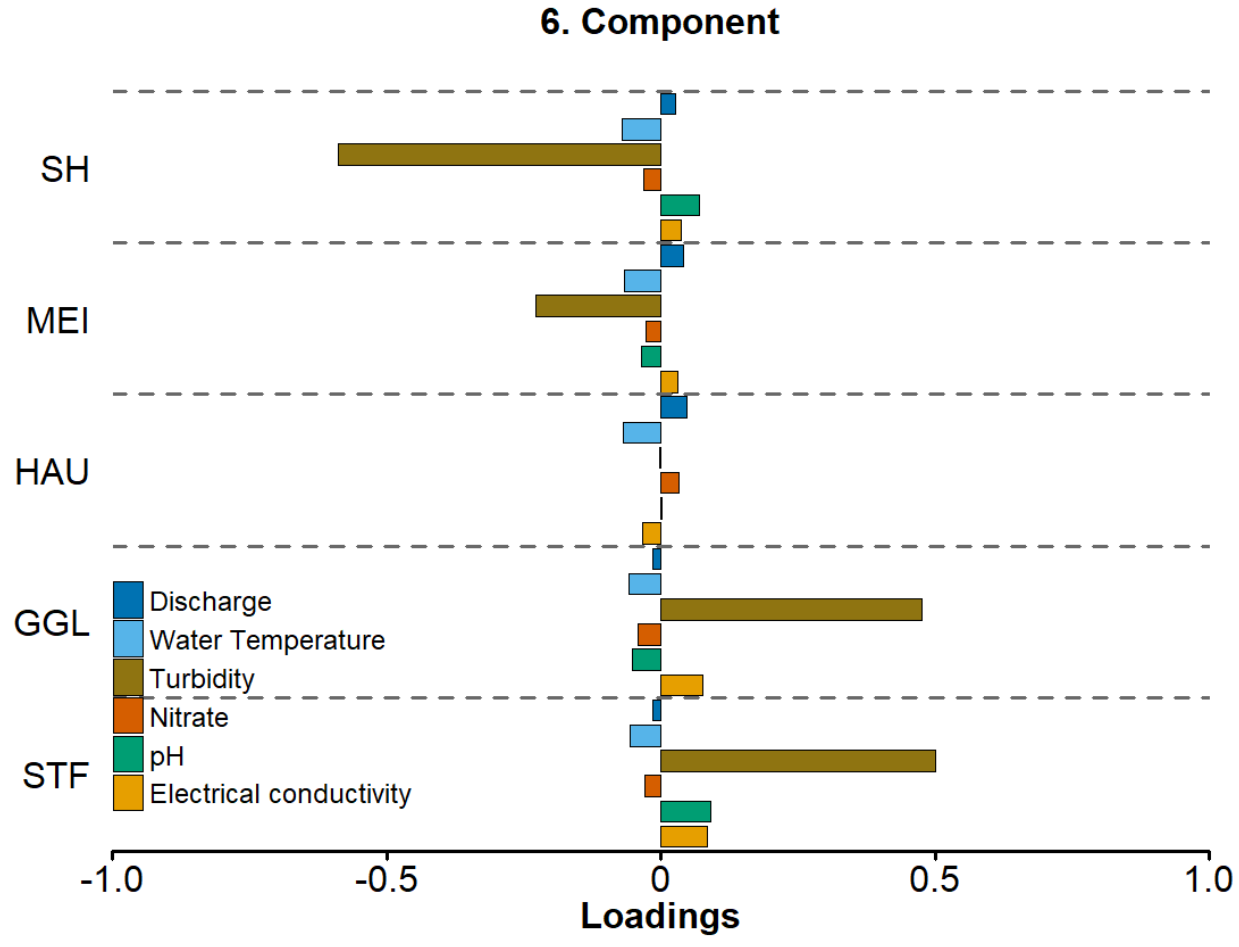

Figure 12. Loadings on the sixth principal component (PC6) for water quality variables across five sampling sites.

https://doi.org/10.5194/egusphere-2026-1203
Preprint. Discussion started: 9 April 2026

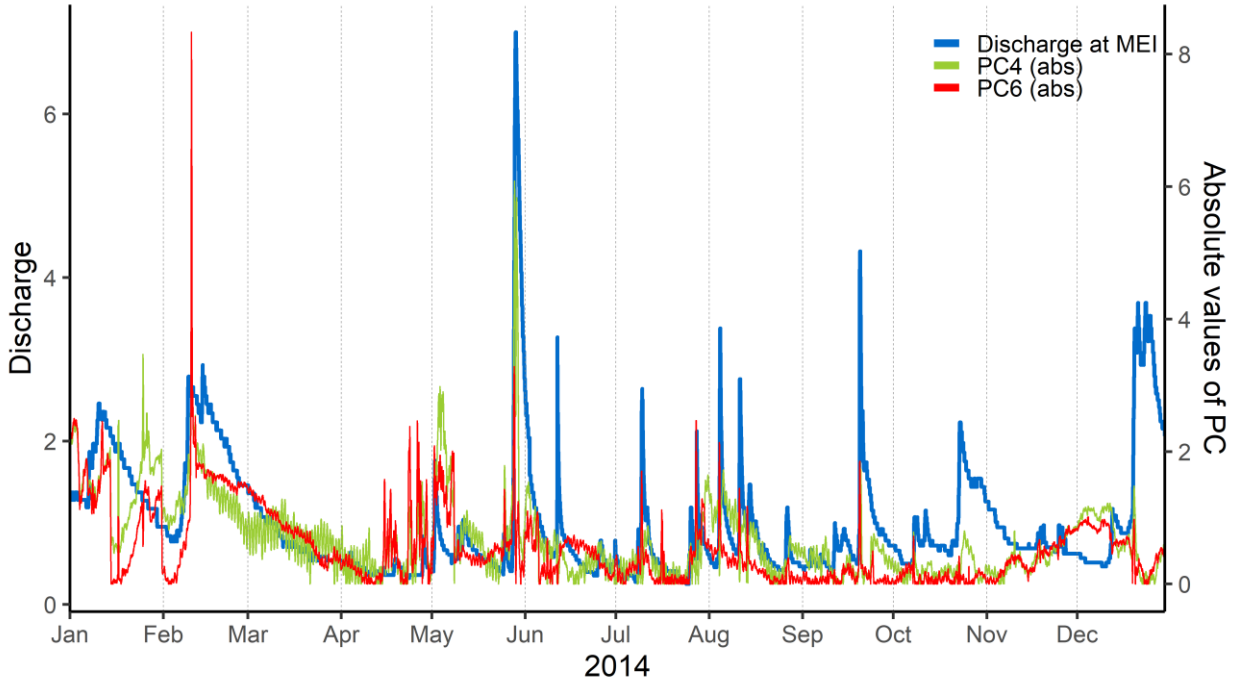

Figure 13. Time series of discharge at GGL and scores of PC4 and PC6 during 2014.

4.6 Seventh component

Figure 14 illustrates that most variables show little correlation with the loadings of the seventh principal component (PC7), indicating that this component is less influential for most parameters. The only major exception is pH at SH station, with a correlation exceeding 0.5. Obviously PC7 is capturing localized processes that specifically affect pH dynamics at SH.

The time series in Figure 15 highlights coinciding peaks of very high pH values (>9.5) at SH during specific periods, including the first half of 2016, the summer of 2018, and spring to early summer of 2019. These elevated pH levels appear to be linked to the efflux of the acid mine drainage treatment plant located on the Uhlenbach stream, a tributary of the Selke River, which flows into the Selke approximately 550 meters upstream of the SH gauging station. The treatment plant efflux contributes a discharge of about 180 m³/h, representing 4% of the mean Selke discharge at SH (1.09 m³/s or 3924 m³/h) but a significantly larger proportion (250%) of the minimum Selke discharge (0.02 m³/s or 72 m³/h). This contribution during lowflow conditions likely rise the plant's influence on the river's pH levels at SH.

https://doi.org/10.5194/egusphere-2026-1203
Preprint. Discussion started: 9 April 2026

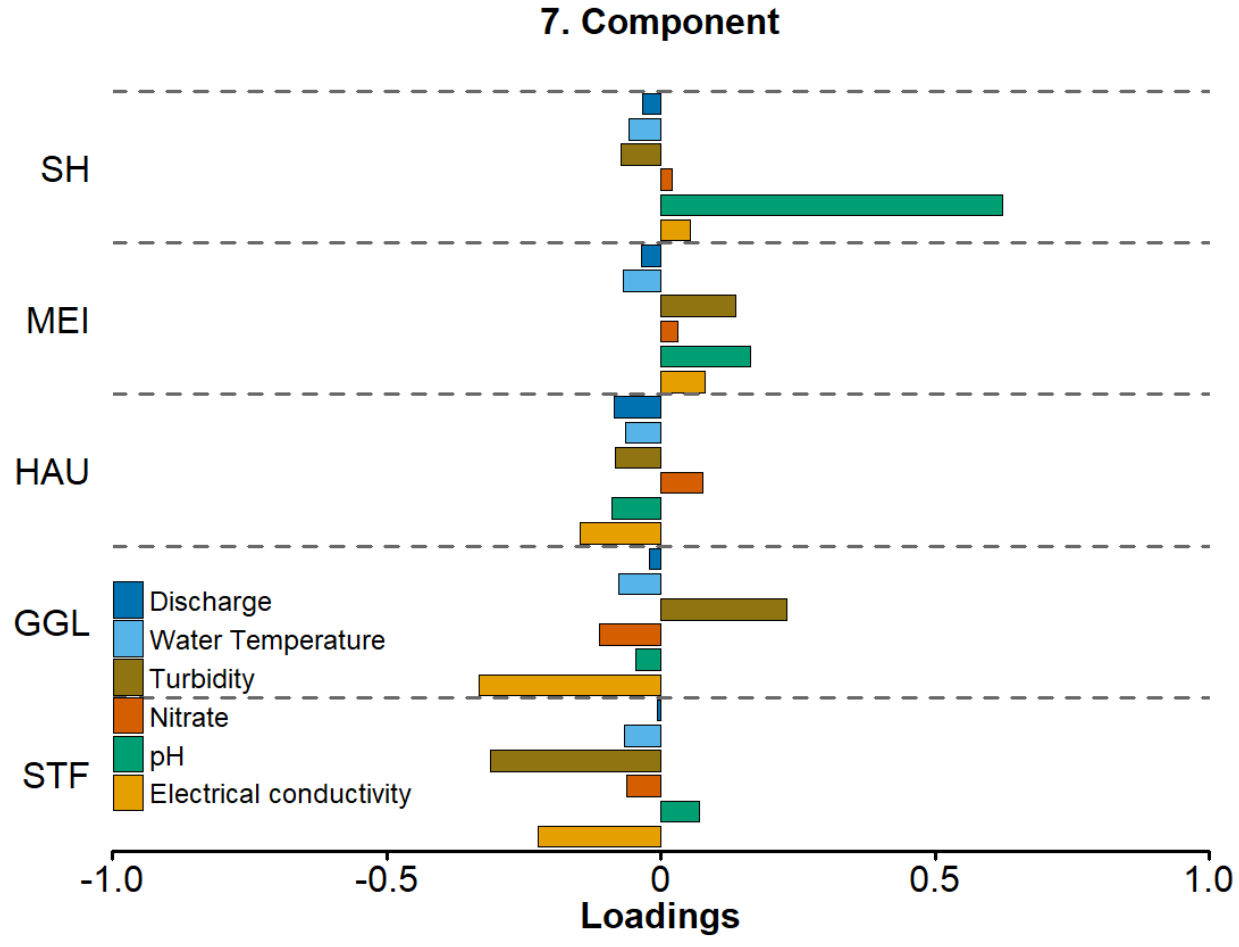

Figure 14. Loadings on the seventh principal component (PC7) for water quality variables across five sampling sites.

https://doi.org/10.5194/egusphere-2026-1203
Preprint. Discussion started: 9 April 2026

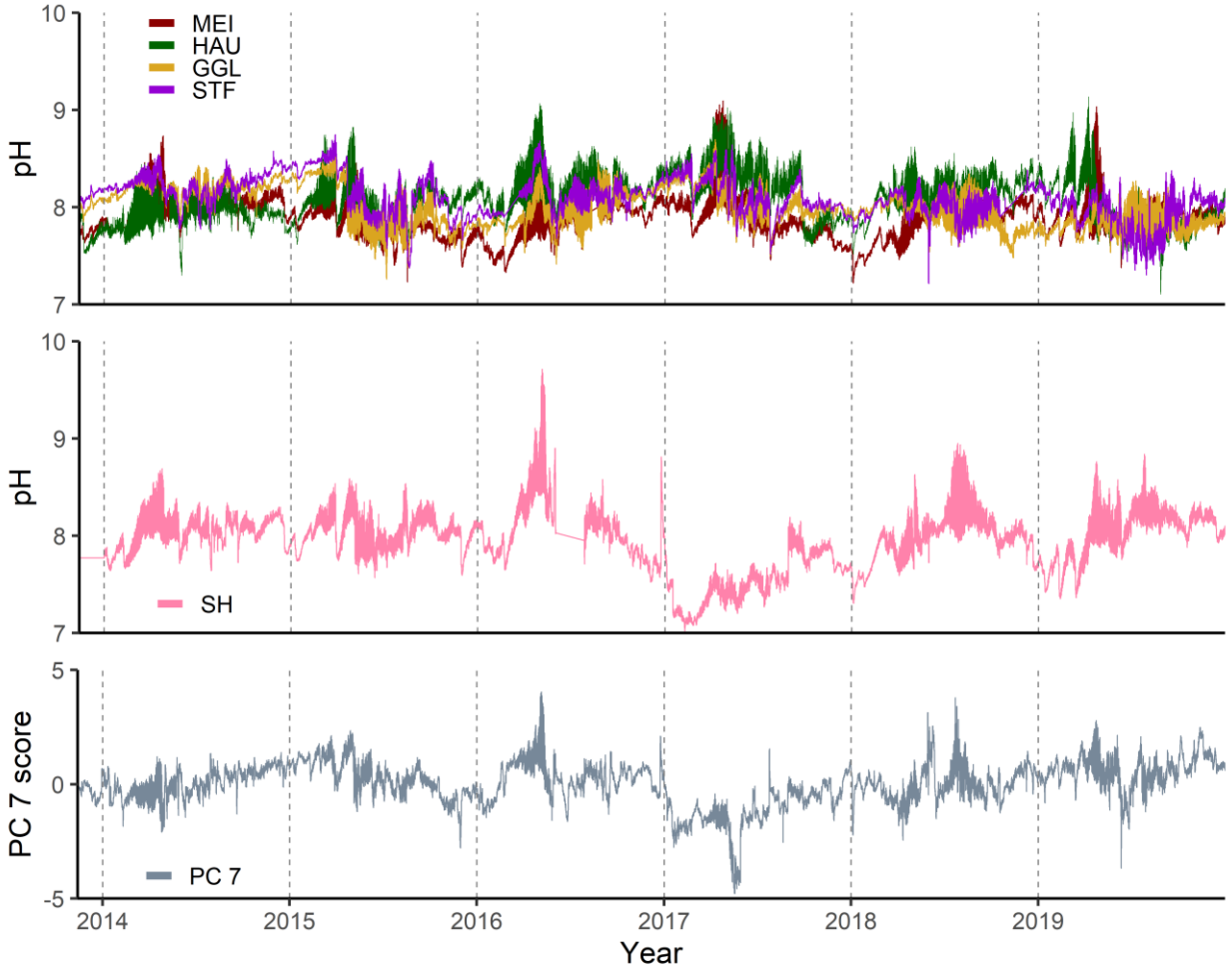

Figure 15. Comparison of the observed pH time series with the PC7 scores. The top panel shows the pH values for stations MEI, HAU, GGL and STF, the middle panel pH observed at station SH, and the lower panel the PC7 time series.

4.7 Eighth component

The loadings graph of PC8 (Fig. 16) reveals a mix of mostly weak positive and negative correlations between variables at the three upstream monitoring stations. In contrast, at the two stations located in the lower catchment, all variables exhibit positive correlations with this component. Among these variables, nitrate exhibits the highest correlation, indicating that this component is particularly sensitive to nitrate dynamics in the lower catchment.

The analysis of the PC8 time series reveals a subtle yet distinct seasonal pattern compared to PC1. While PC1 primarily represents the long-term dynamics resulting from the mixing of shallow polluted groundwater and deeper, less polluted groundwater, PC8 appears sensitive to shorter-term dynamics associated with intermediate-depth discharge to the river. Figure 17 illustrates this effect by zooming into the year of 2015 as an example. In general, the seasonal pattern of PC8 scores is closely related to that of nitrate concentration at GGL and STF. This seasonal trend likely reflects the combined effects of

https://doi.org/10.5194/egusphere-2026-1203
Preprint. Discussion started: 9 April 2026

agricultural runoff, plant uptake, and microbial activity. During spring, increased agricultural activity and fertilizer application contribute to higher nitrate levels, while plant growth and microbial denitrification processes reduce concentrations later in the season. However, in the first phase of sharp nitrate concentration peaks like in early April, in August and in late November/ early December 2015 PC8 scores peak sharply downwards, indicating strong dilution effects of fresh water in the rising limb of the hydrograph. Likewise, dilution effects can explain the negative correlation between PC8 and turbidity at HAU, that is, downstream the outflow of a wastewater treatment plant.

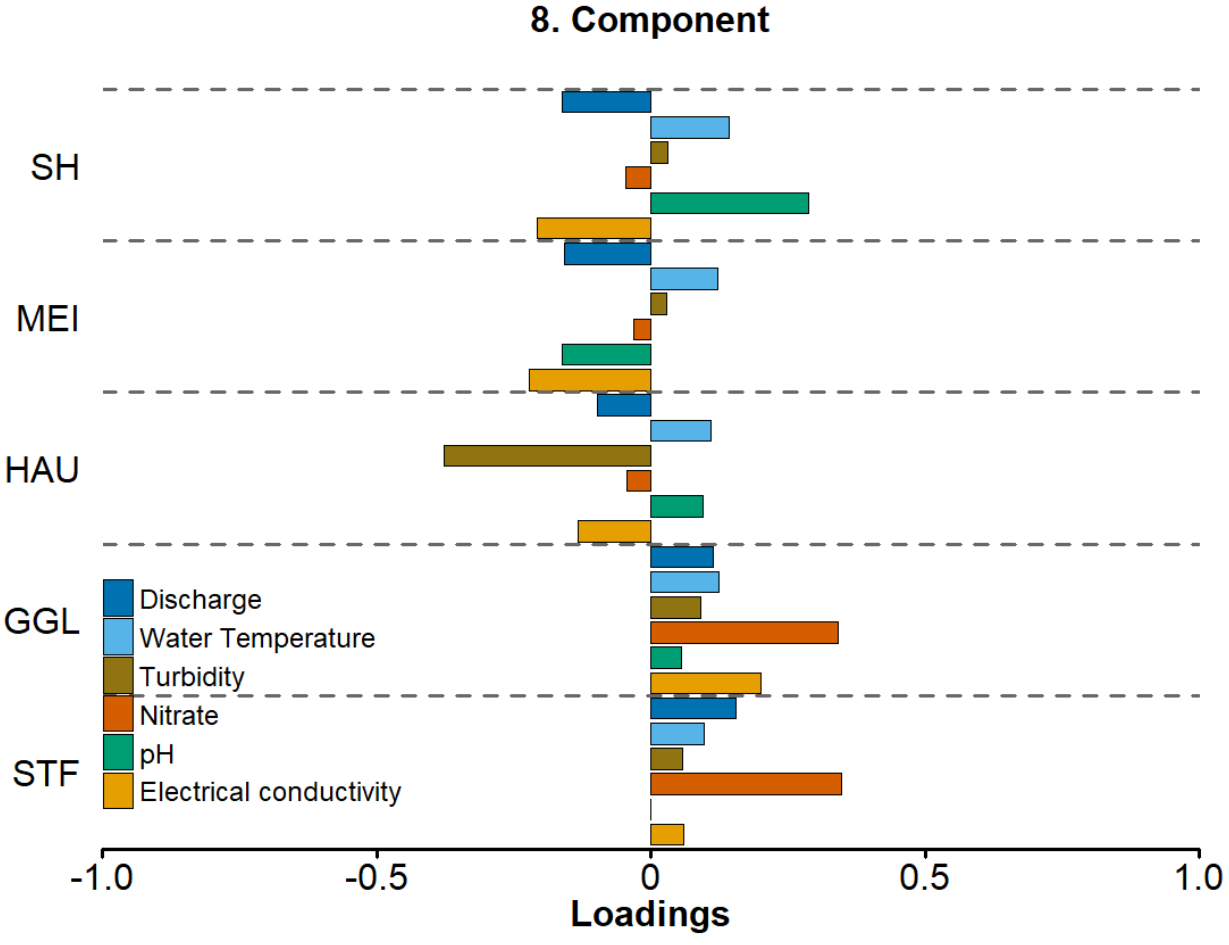

Figure 16. Loadings on the eighth principal component (PC8) for water quality variables across the five sampling sites.

https://doi.org/10.5194/egusphere-2026-1203
Preprint. Discussion started: 9 April 2026

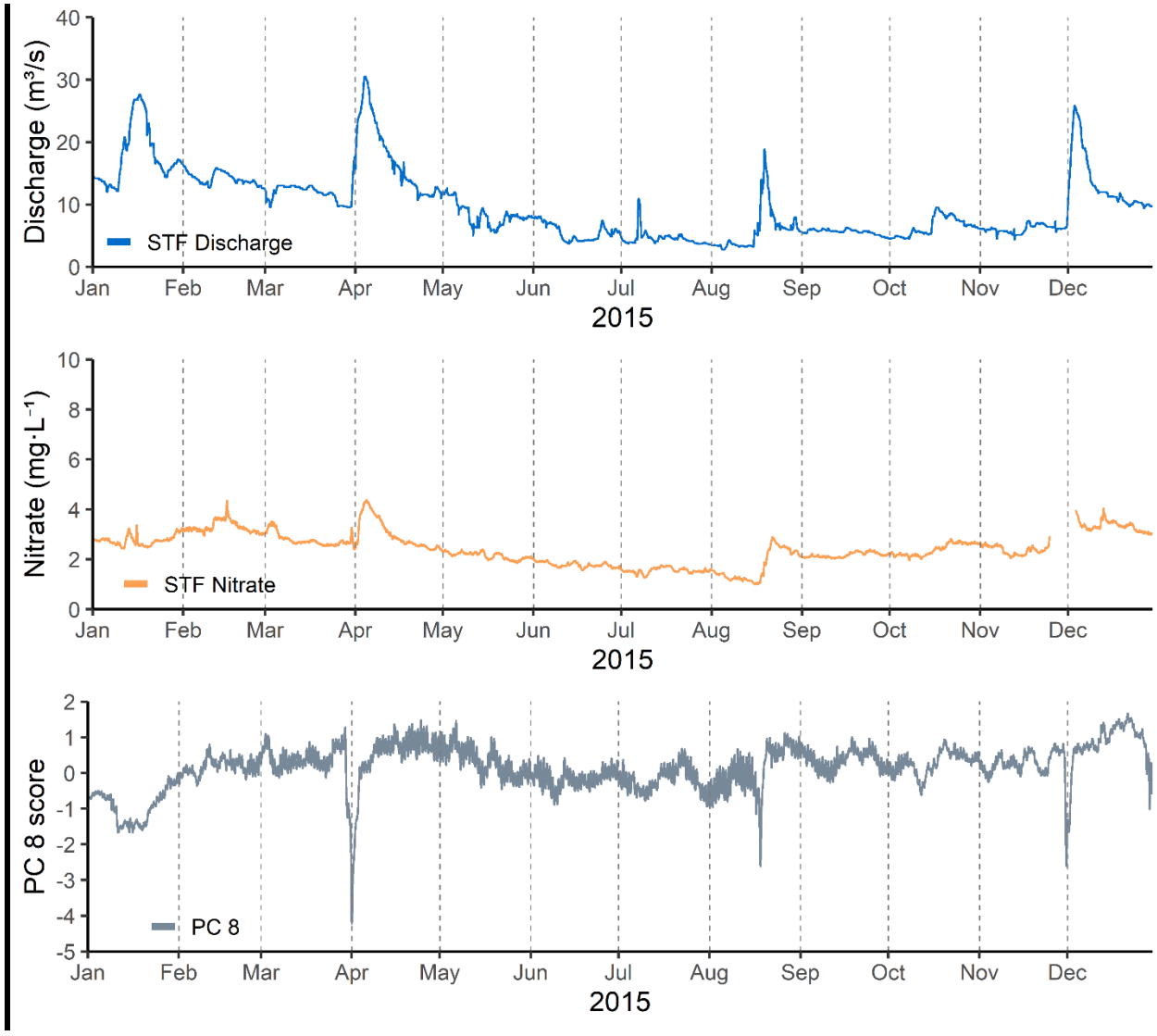

Figure 17. Time series of PC8 scores and nitrate concentration at the STF station for 2015.

5 Discussion

Principal component analysis was used to identify and differentiate between different phenomena affecting stream water quality at different sites along the Selke and Bode River. The rationales and associated uncertainties are discussed in the following. These need to account for hydrological processes, in particular for major differences between the upland and the lowland part of the catchment which are discussed first.

https://doi.org/10.5194/egusphere-2026-1203
Preprint. Discussion started: 9 April 2026

5.1 Hydrological processes

Although subcatchment size increases considerably along the stream, discharge remains relatively constant at SH, MEI, and HAU, as well as at GGL and STF. There are several reasons for this: Firstly, precipitation is significantly higher in the mountainous region compared to the lowlands, where groundwater recharge is very low. Secondly, the acid mine drainage treatment plant upstream of SH introduces substantial volumes of water from several interconnected mines, potentially draining an area that extends beyond the Selke catchment.

Thirdly, part of the Selke's flow is diverted to fill the former open pit at Nachterstedt (Winter et al. 2021). Fourthly, the stream features both gaining and losing reaches, where inflows and outflows may compensate each other (Zhang et al., 2020). As a result, net streamflow does hardly increase downstream of MEI. In contrast, water quality changes as upstream water is gradually replaced by downstream sources, a pattern confirmed by PCA results.

Despite these scenarios, Principal Component Analysis provides evidence of additional, albeit episodic, discharge contributions at short time scales. Specifically, PCA components PC2 and PC8 indicate instances of additional discharge inputs to the stream during short periods, suggesting intermittent groundwater or surface runoff contributions even when overall net groundwater recharge may be minimal.

5.2 PC1: Discharge peaks

During peak discharge events, river water composition changes significantly due to the rapid influx of surface soil solutions and shallow groundwater. Consequently, nitrate export from agricultural areas to the streams increases during these events. Several studies have demonstrated that preferential flow paths activated during storm events can bypass natural soil buffers, posing risks to water quality (Lischeid et al., 2002). Furthermore, runoff events hydrologically connect riparian zones to streams, shifting water chemistry and highlighting the spatial and temporal complexity of hydrological connectivity documented in various catchments (Weyer et al., 2014). While some catchments exhibit nitrate dilution with increasing discharge, the relationship is often complex (Neal et al., 2012). Our study, for example, reveals a clear 'mobilization' pattern of pre-event water with high nitrate concentration thus increasing stream nitrate concentration with discharge.

Results indicate that higher discharge is the primary factor driving nitrate mobilization, likely due to enhanced hydrological connectivity and surface runoff during highflow events. The concept that discharge peaks activate the hydrological connectivity of the catchment area and mobilize nitrates from terrestrial sources is a fundamental mechanism driving nitrate discharge. This is supported by studies in other complex geological systems, such as karst catchments, where it has also been found that prevailing conditions and precipitation characteristics (identified by a PCA of event metrics) are the primary drivers of nitrate loading during rainfall events (Yue et al, 2023).

This behavior is confirmed by Zhang et al. (2020) and Winter et al. (2021), who found that nitrate export in the Selke subcatchment is affected by groundwater contributions and streamflow variability. This interpretation is reinforced by the

https://doi.org/10.5194/egusphere-2026-1203
Preprint. Discussion started: 9 April 2026

correlation analysis of the raw data, which shows a strong negative correlation between flow (Q) and electrical conductivity (EC) and a positive correlation with nitrate (NO_3) (Fig. S1, S2 and S3).

Although nitrate uptake increases during warm periods, the consistent positive correlation between nitrate concentration and discharge across all stations suggests that dilution does not explain the seasonal variability. Instead, it appears that nitrate mobilization from terrestrial sources is primarily governed by hydrological connectivity rather than biological processing alone. This pattern is consistent with the findings of Rode et al. (2016), which demonstrated that groundwater head controls nitrate export in lowland agricultural catchments. Additionally, studies in the Bode River Catchment indicate that while higher temperatures promote denitrification, these processes are insufficient to offset the external influx of nitrates, revealing a persistent contamination source, especially in areas where nitrate-rich groundwater contributes to baseflow (Mueller et al., 2016; Musolff et al., 2016).

5.3 PC2: Subsurface saline contributions

The second principal component (PC2) highlights a separate dimension of spatiotemporal variability in the river system, focusing especially on electrical conductivity (EC) in the downstream reach. The negative correlation of discharge, temperature, and turbidity with PC2 suggests that, under lowflow or reduced surface-runoff scenarios, the other variables (pH, nitrate, and especially EC) take relevance in driving the system's variation. Such an increase in EC during lowflow conditions is often observed in river systems, as groundwater contribution with higher dissolved solids becomes more dominant and dilution decreases. This is consistent with the weak positive loadings of EC on PC2 (Fig. 5).

For the two downstream sites, however, the effect is much more prominent. This result aligns with the descriptions of the Bode catchment made by Luo et al. (2011), which demonstrate how saline upwelling from flooded salt mines influences regional groundwater and surface water salinity. This effect is influenced by both geological factors and historical mining activities that have altered groundwater movement. Luo et al. (2011) demonstrate that a flooded salt mine in Staßfurt (STF) has been a long-term source of saline groundwater migration into adjacent aquifers, contributing to regional groundwater salinization. Similarly, Brandes et al. (2012) highlight the role of the Helmstedt-Staßfurt salt wall in redirecting groundwater flow, allowing saline upwelling to influence surface waters.

5.4 PC3: In-stream photosynthesis

The third principal component (PC3) primarily captures variability in pH dynamics, particularly in the downstream stations GGL and STF. An examination of daily pH variations reveals a distinct diurnal cycle, where pH increases during daylight hours and decreases at night. This process, driven by the balance between daytime photosynthesis and nighttime respiration, has been identified as the primary factor in daily pH variation in a wide range of rivers, including those affected by mine drainage in North America (Gammons et al., 2007). Rode et al. (2016) encountered that oxygen daily amplitudes were closely correlated with pH daily amplitudes in the Selke subcatchment. Studies by Demars et al. (2011) and Halbedel et al. (2013)

https://doi.org/10.5194/egusphere-2026-1203
Preprint. Discussion started: 9 April 2026

support the role of dissolved oxygen in water released by photosynthetic activity, and how CO_2 uptake by photosynthesis increases pH in circum-neutral freshwater systems.

In addition to the diurnal cycle, Figure 9 also reveals a seasonal pattern, showing an initial increase in the amplitude of PC3 during spring, followed by a second increase at the beginning of summer. This pattern is consistent with the findings of Huang et al. (2022), where the simulation of gross primary production (GPP) also exhibited a first peak in spring, linked to phytoplankton chlorophyll-a concentrations, and a second peak in summer, associated with benthic algae biomass.

The dominance of PC3 in the downstream stations suggests that limited riparian canopy conditions in these areas foster phytoplankton, phytobenthos or periphyton growth, thereby amplifying the photosynthetic effect on pH. The wide valley morphology, lower flow velocities, and reduced canopy shading create an optimal environment for algal proliferation, this has been observed in other catchments in studies like Sabater et al. (2008) and Halliday et al. (2016).

Attributing this component to in-stream photosynthesis addresses a complex issue. Although the amplitude of PC3 shows not only a clear diurnal but a seasonal pattern as well suggesting a link with biological activity (Fig. 9), seasonal correlation analysis (Fig. S2) reveals that the relationship between pH and water temperature does not follow a simple pattern, varying greatly between sites and seasons. This suggests that, although temperature is an influential factor, other elements such as light availability, nutrients, and ecosystem respiration also significantly modulate pH, and PC3 captures the net effect of these diurnal processes.

5.5 PC4, PC5 and PC6: Sources of turbidity

The fourth component, characterized by strong positive loadings of turbidity at all sites and limited correlation with other variables, pointing to limited contribution of the other variables to the process that affect turbidity. This is consistent with findings from studies conducted within the Bode hydrological observatory, where sediment transport processes have been found to operate independently from other water quality parameters under certain hydrological conditions like brief intensive episodes (Wollschläger et al., 2017; Horowitz, 2013).

The fifth component presents an interesting case where turbidity correlations vary across sites, notably displaying a strongly negative correlation at the HAU station while remaining weakly positive at other locations. Given the proximity of HAU to a wastewater treatment plant (Winter et al., 2021), the dilution effect of treated water during peak flow conditions could influence these correlations. The high positive correlation of this component for pH further supports the hypothesis that wastewater effluent alters the water quality downstream.

The sixth component exhibits a spatially differing correlation pattern, transitioning from strongly negative upstream to strongly positive downstream. This suggests a gradient of influence from localized sediment sources and hydrological processes that evolve along the river continuum. Similar findings have been reported in studies assessing nitrate and sediment retention dynamics during drought conditions, where sediment mobilization mechanisms differ between headwater and downstream reaches.

https://doi.org/10.5194/egusphere-2026-1203
Preprint. Discussion started: 9 April 2026

The loess lowland areas are much more prone to sediment losses by surface runoff and riverbank erosion than forested lower mountain range areas (Abbas et al. 2024). This component likely encapsulates interactions between bank erosion, surface runoff, and potential inputs from road drainage, reinforcing the heterogeneous nature of sediment transport across different hydrological conditions (Rode and Suhr, 2007; Walling et al., 1992).

5.6 PC7: Anthropogenic influence on pH variability

The seventh principal component (PC7) shows a distinct correlation primarily with pH at the SH station, indicating that it captures specific localized processes influencing pH dynamics uniquely at this location. Time series reveal periodic spikes in pH (>9.5), particularly noticeable during lowflow periods in 2016, 2018, and 2019. These pronounced variations in pH are likely associated with anthropogenic inputs, specifically effluent discharge from the acid mine drainage (AMD) treatment facility located upstream of the SH station on the Uhlenbach tributary.

Acidic mine water is produced naturally through the oxidation of sulfidic ores, abundant in the fluorspar mines of the Harz Mountains. To mitigate this acidity, active treatment is applied by adding alkaline substances, mainly hydrated lime ($Ca(OH)_2$), resulting in the precipitation of metals as hydroxides and generation of low-density sludge (LDS) enriched in iron oxyhydroxides and residual carbonate (Kubiak and Wolkersdorfer, 2008). The importance of this treatment plant resides in its operability, considering that it has a maximum treatment capacity of approximately 0.3 m^3/s (equivalent to 1080 m^3/h), in accordance with verbal communication with plant personnel (September 7, 2017). The discharge at the SH station shows an uneven distribution, with an average discharge of 0.67 m^3/s but a much lower median of 0.38 m^3/s. In this context, the river flow falls below the plant's maximum treatment capacity for approximately 40% of the observation period, indicating that, under low flow conditions, the treated effluent may constitute a substantial fraction of the total river flow.

The PCA's ability to isolate a signal as specific and localized as the intermittent effluent from the acid mine drainage treatment plant (PC7) demonstrates the power of this method for detecting point sources of pollution. This is a key objective in water quality management, and other studies have also successfully used multivariate statistical approaches to identify the signature of specific effluents in complex datasets. For example, Shrestha and Kazama (2007) applied PCA to identify sources of pollution in the Fuji River basin in Japan and were able to attribute a specific component to the thermal and chemical signature of industrial effluents from paper mills. Similarly, PC7 effectively captures the unique chemical fingerprint of the treatment plant, distinguishing it from all other natural and diffuse sources of variability in the river.

5.7 PC8: Downstream nitrate patterns

PC8 is particularly sensitive to nitrate dynamics in the lower basin (GGL and STF). Note that PC8 explains part of the streamwater quality dynamics that is not already grasped by PC1 to PC7. Correspondingly the seasonal pattern of PC8 with maximum scores in spring and a clear decline during the growing season (Fig. 17) indicates that at sites with positive loadings like GGL and STF these seasonal effects are stronger compared to the remaining sites (SH, MEI, HAU) with predominantly negative, albeit weak loadings (Fig. 16).

https://doi.org/10.5194/egusphere-2026-1203
Preprint. Discussion started: 9 April 2026

This seasonal behavior reflects significant nitrate enrichment associated with intensive agricultural activities prevalent in the lower basin, where slow flowing lowland streams are heavily impacted by agricultural runoff. These agricultural influences typically lead to high nitrate concentrations (7–50 mg L^{-1}) and elevated $\delta^{15}N\text{-}NO_3$ values, attributable primarily to nitrification processes of ammonium-based fertilizers (Mueller et al., 2016). Furthermore, nitrate from agricultural fertilizers is particularly susceptible to mobilization and subsequent wash-out during rainfall events, significantly contributing to stream nitrate loads. However, this seasonal trend is complemented by a contrasting short-term dilution effect during discharge peaks. Such dilution, marked by sharp negative peaks in nitrate concentration coinciding with increased discharge, initially appears counterintuitive because highflow events are often associated with increased nitrate inputs. The beginning of highflow event is often dominated by surface runoff which is low in nitrate concentration. Nitrate concentrations are mostly increasing when interflow, which is leaching the soil column, is becoming the dominant flow component later during the event Dupas et al. (2016). Yet, this dilution phenomenon can be explained by the rapid input of less nitrate-rich intermediate-depth discharge waters into the river system, temporarily lowering nitrate concentrations despite increased flow. Thus, PC8 captures both the seasonal enrichment dynamics due to biological and agricultural processes, and the short-term dilution effects associated with hydrological events, clearly distinguishing it from the groundwater-driven, long-term nitrate dynamics represented by PC1.

Although this study demonstrates the ability of PCA to disentangle complex processes from high-frequency data, there are promising future research approaches that could provide even greater validation and detail. On the one hand, a specific analysis based on hydrological events would allow for confirmation of the interpretations of the components associated with runoff (PC1, PC4-6), linking them more directly to specific flow paths such as surface runoff or bank erosion during floods. On the other hand, a multi-temporal scale analysis, applying aggregation techniques to the data, could serve to evaluate the stability of the component loads and determine which processes dominate at different temporal resolutions. But note that some PC (PC1, PC3) would not have been possible to understand without a sub-daily temporal resolution.

6 Conclusions

The application of Principal Component Analysis (PCA) to high-resolution multivariate data has proven to be an effective tool for identifying the complex and diverse factors influencing water quality in the Bode River basin. The high-resolution time series made it possible to detect rapid and transient processes and attribute them to specific physical, biogeochemical or anthropogenic factors.

By reducing the dataset's dimensionality, PCA decomposes coherent spatiotemporal patterns into distinct spatial and temporal series, offering deeper insight into the processes affecting water quality at both catchment-wide and local scales. This method provides a robust statistical framework for isolating signals within the dataset and distinguishing systematic variability from random noise based on their temporal characteristics.

Furthermore, as a data-adaptive technique, PCA relies solely on the intrinsic properties of the observational data, requiring no prior assumptions or subjective input. Consistent with findings by Pasari (2022), this study confirms PCA as a state-of-the-art

https://doi.org/10.5194/egusphere-2026-1203
Preprint. Discussion started: 9 April 2026

approach for detecting, estimating, and predicting short-term, small-scale, and long-term variations within complex environmental datasets.

The successful interpretation of the principal components in this study was greatly aided by the substantial body of research available for the study region. This raises an important point about the method's generalizability. While detailed background knowledge is crucial for the final interpretation and labelling of the processes, the PCA method itself remains a powerful tool for the initial detection and separation of dominant statistical patterns in any complex dataset. In a catchment without such a wealth of environmental background information, this approach can therefore be used to identify the key underlying patterns of variability, which can then guide the formulation of data-driven hypotheses and the design of more targeted and efficient field investigations.

This study underscores the value of integrating high-resolution temporal and spatial data with multivariate techniques to enhance watershed management. The incorporation of statistical and modelling approaches, including PCA, can be further complemented with hydrogeochemical simulations. Future research could expand on this framework by integrating PCA with hydrological models or machine learning to predict system responses under climate change and land-use modification scenarios. Overall, this research highlights the potential of multivariate analytics for deciphering and quantifying complex interactions regulating water quality in heterogeneous and human-impacted catchments.

Data availability

Data will be made available on request.

CRediT authorship contribution statement

Kenneth Gutiérrez-García: Writing – review & editing, Writing – original draft, Validation, Software, Methodology, Investigation, Formal analysis, Data curation, Conceptualization. **Gunnar Lischeid:** Writing – review & editing, Writing – original draft, Validation, Supervision, Software, Resources, Methodology, Investigation, Formal analysis, Conceptualization, Funding acquisition. **Michael Rode:** Writing – review & editing, Resources, Data curation.

Declaration of competing interest

The authors declare no conflict of interest.

Disclaimer

Copernicus Publications remains neutral with regard to jurisdictional claims made in the text, published maps, institutional affiliations, or any other geographical representation in this paper. While Copernicus Publications makes every effort to include

appropriate place names, the final responsibility lies with the authors. Views expressed in the text are those of the authors and do not necessarily reflect the views of the publisher

Acknowledgements

Kenneth Gutiérrez-García and Gunnar Lischeid would like to thank Michael Rode, the Helmholtz Centre for Environmental Research-UFZ and the TERENO observational facilities for providing access to the high-frequency water quality data.

Funding

This research was supported by the project ISO-SCALE funded by the Leibniz Collaborative Excellence (SAW K444/2022).

References

Abbas, G., Jomaa, S., Fink, P., Brosinsky, A., Nowak, K. M., Kümmel, S., Schkade, U., and Rode, M.: Investigating sediment sources using compound-specific stable isotopes and conventional fingerprinting methods in an agricultural loess catchment, CATENA, 246, 108336, https://doi.org/10.1016/j.catena.2024.108336, 2024.

Altermann, M., Rinklebe, J., Merbach, I., Körschens, M., Langer, U., and Hofmann, B.: Chernozem—Soil of the Year 2005, J. Plant Nutr. Soil Sci., 168, 725–740, https://doi.org/10.1002/jpln.200521814, 2005.

Anders, T., Hetzer, J., Knapp, N., Forrest, M., Langan, L., Tölle, M. H., Wellbrock, N., and Hickler, T.: Modelling past and future impacts of droughts on tree mortality and carbon storage in Norway spruce stands in Germany, Ecol. Model., 501, 110987, https://doi.org/10.1016/j.ecolmodel.2024.110987, 2025.

Brandes, C., Pollok, L., Schmidt, C., Wilde, V., and Winsemann, J.: Basin modelling of a lignite-bearing salt rim syncline: insights into rim syncline evolution and salt diapirism in NW G ermany, Basin Res., 24, 699–716, https://doi.org/10.1111/j.1365-2117.2012.00544.x, 2012.

Chapman, D. V. and Sullivan, T.: The role of water quality monitoring in the sustainable use of ambient waters, One Earth, 5, 132–137, https://doi.org/10.1016/j.oneear.2022.01.008, 2022.

Chen, M., Jomaa, S., Lausch, A., Beudert, B., Ghaffar, S., Jia, W., and Rode, M.: Impact of Forest Dieback on Hydrology and Nitrogen Export Using a New Dynamic Water Quality Model, Water Resour. Res., 60, e2024WR037341, https://doi.org/10.1029/2024WR037341, 2024.

Chen, Z., Zhang, S., Coster, A. J., and Fang, G.: EOF analysis and modeling of GPS TEC climatology over North America, J. Geophys. Res. Space Phys., 120, 3118–3129, https://doi.org/10.1002/2014JA020837, 2015.

https://doi.org/10.5194/egusphere-2026-1203
Preprint. Discussion started: 9 April 2026

Demars, B. O. L., Russell Manson, J., Ólafsson, J. S., Gíslason, G. M., Gudmundsdóttir, R., Woodward, G., Reiss, J., Pichler, D. E., Rasmussen, J. J., and Friberg, N.: Temperature and the metabolic balance of streams: Temperature and the metabolic balance of streams, Freshw. Biol., 56, 1106–1121, https://doi.org/10.1111/j.1365-2427.2010.02554.x, 2011.

Di, C., Yang, X., and Wang, X.: A Four-Stage Hybrid Model for Hydrological Time Series Forecasting, PLoS ONE, 9, e104663, https://doi.org/10.1371/journal.pone.0104663, 2014.

Diamantini, E., Lutz, S. R., Mallucci, S., Majone, B., Merz, R., and Bellin, A.: Driver detection of water quality trends in three large European river basins, Sci. Total Environ., 612, 49–62, https://doi.org/10.1016/j.scitotenv.2017.08.172, 2018.

Diercks, M.-L., Stanek, K., Domínguez-Gonzalez, L., and Ehling, B.: Quaternary landscape evolution and tectonics in Central Germany – A case study of the Harz, Geomorphology, 388, 107794, https://doi.org/10.1016/j.geomorph.2021.107794, 2021.

Dupas, R., Jomaa, S., Musolff, A., Borchardt, D., and Rode, M.: Disentangling the influence of hydroclimatic patterns and agricultural management on river nitrate dynamics from sub-hourly to decadal time scales, Sci. Total Environ., 571, 791–800, https://doi.org/10.1016/j.scitotenv.2016.07.053, 2016.

CORINE Land Cover: https://land.copernicus.eu/en/products/corine-land-cover, last access: 5 March 2026.

Gammons, C. H., Milodragovich, L., and Belanger-Woods, J.: Influence of diurnal cycles on metal concentrations and loads in streams draining abandoned mine lands: an example from High Ore Creek, Montana, Environ. Geol., 53, 611–622, https://doi.org/10.1007/s00254-007-0676-z, 2007.

Gewers, F. L., Ferreira, G. R., de Arruda, H. F., Silva, F. N., Comin, C. H., Amancio, D. R., and Costa, L. da F.: Principal Component Analysis: A Natural Approach to Data Exploration, https://doi.org/10.48550/ARXIV.1804.02502, 2018.

Halbedel, S., Büttner, O., and Weitere, M.: Linkage between the temporal and spatial variability of dissolved organic matter and whole-stream metabolism, Biogeosciences, 10, 5555–5569, https://doi.org/10.5194/bg-10-5555-2013, 2013.

Halliday, S. J., Skeffington, R. A., Wade, A. J., Bowes, M. J., Read, D. S., Jarvie, H. P., and Loewenthal, M.: Riparian shading controls instream spring phytoplankton and benthic algal growth, Environ. Sci. Process. Impacts, 18, 677–689, https://doi.org/10.1039/C6EM00179C, 2016.

Hannachi, A., Jolliffe, I. T., and Stephenson, D. B.: Empirical orthogonal functions and related techniques in atmospheric science: A review, Int. J. Climatol., 27, 1119–1152, https://doi.org/10.1002/joc.1499, 2007.

Horowitz, A. J.: A Review of Selected Inorganic Surface Water Quality-Monitoring Practices: Are We Really Measuring What We Think, and If So, Are We Doing It Right?, Environ. Sci. Technol., 47, 2471–2486, https://doi.org/10.1021/es304058q, 2013.

Huang, J., Borchardt, D., and Rode, M.: How do inorganic nitrogen processing pathways change quantitatively at daily, seasonal, and multiannual scales in a large agricultural stream?, Hydrol. Earth Syst. Sci., 26, 5817–5833, https://doi.org/10.5194/hess-26-5817-2022, 2022.

Hyndman, R., Athanasopoulos, G., Caceres, G., Chhay, L., Kuroptev, K., Mücke, M., O'Hara-Wild, M., Petropoulos, F., Razbash, S., and Wang, E.: _forecast: Forecasting functions for time series and linear models_, 2023.

https://doi.org/10.5194/egusphere-2026-1203
Preprint. Discussion started: 9 April 2026

Jolliffe, I. T.: Principal Component Analysis: A Beginner's Guide I. Introduction and application., Weather, 45, 375–382, https://doi.org/10.1002/j.1477-8696.1990.tb05558.x, 1990.

Jolliffe, I. T. and Cadima, J.: Principal component analysis: a review and recent developments, Philos. Trans. R. Soc. Math. Phys. Eng. Sci., 374, 20150202, https://doi.org/10.1098/rsta.2015.0202, 2016.

Kim, K.-Y. and Wu, Q.: A Comparison Study of EOF Techniques: Analysis of Nonstationary Data with Periodic Statistics, J. Clim., 12, 185–199, https://doi.org/10.1175/1520-0442-12.1.185, 1999.

Kleine-Kleffmann, U.: The discovery of the first potash mine and the development of the potash industry since 1861, J. Plant Nutr. Soil Sci., 186, 615–622, https://doi.org/10.1002/jpln.202300382, 2023.

Kröcher, J., Ghazaryan, G., and Lischeid, G.: Unravelling Regional Water Balance Dynamics in Anthropogenically Shaped Lowlands: A Data-Driven Approach, Hydrol. Process., 39, e70053, https://doi.org/10.1002/hyp.70053, 2025.

Kubiak, C. and Wolkersdorfer, C.: Low Density Sludge Storage In A Flooded Underground Mine, in: IMWA Congress, IMWA Congress, Carlsbad, Czech Republic, 2008.

Lehr, C. and Lischeid, G.: Efficient screening of groundwater head monitoring data for anthropogenic effects and measurement errors, Hydrol. Earth Syst. Sci., 24, 501–513, https://doi.org/10.5194/hess-24-501-2020, 2020.

Li, Y., Yang, X., Lischeid, G., Wollheim, W. M., Jomaa, S., Zhou, X., and Rode, M.: Responses of Wetted River Network Contraction and Expansion Dynamics to Prolonged Drought, Water Resour. Res., 61, e2024WR038938, https://doi.org/10.1029/2024WR038938, 2025.

Lischeid, G., Kolb, A., and Alewell, C.: Apparent translatory flow in groundwater recharge and runoff generation, J. Hydrol., 265, 195–211, https://doi.org/10.1016/S0022-1694(02)00108-7, 2002.

Lischeid, G., Balla, D., Dannowski, R., Dietrich, O., Kalettka, T., Merz, C., Schindler, U., and Steidl, J.: Forensic hydrology: what function tells about structure in complex settings, Environ. Earth Sci., 76, 40, https://doi.org/10.1007/s12665-016-6351-5, 2017.

Luo, J., Diersch, H.-J., and Monninkhoff, B.: 3D Modeling of Saline Groundwater Flow and Transport in a Flooded Salt Mine, Staßfurt/Germany, in: Proceedings 2011 Aachen, Germany, 11th International Mine Water Association Congress – Mine Water – Managing the Challenges, 2011.

Meggiorin, M., Bullo, P., Accoto, V., Passadore, G., Sottani, A., and Rinaldo, A.: Applying the Principal Component Analysis for a deeper understanding of the groundwater system: case study of the Bacchiglione Basin (Veneto, Italy), Acque Sotter. - Ital. J. Groundw., 11, 7–17, https://doi.org/10.7343/as-2022-573, 2022.

Mueller, C., Krieg, R., Merz, R., and Knöller, K.: Regional nitrogen dynamics in the TERENO Bode River catchment, Germany, as constrained by stable isotope patterns, Isotopes Environ. Health Stud., 52, 61–74, https://doi.org/10.1080/10256016.2015.1019489, 2016.

Musolff, A., Schmidt, C., Rode, M., Lischeid, G., Weise, S. M., and Fleckenstein, J. H.: Groundwater head controls nitrate export from an agricultural lowland catchment, Adv. Water Resour., 96, 95–107, https://doi.org/10.1016/j.advwatres.2016.07.003, 2016.

https://doi.org/10.5194/egusphere-2026-1203
Preprint. Discussion started: 9 April 2026

Neal, C., Reynolds, B., Rowland, P., Norris, D., Kirchner, J. W., Neal, M., Sleep, D., Lawlor, A., Woods, C., Thacker, S., Guyatt, H., Vincent, C., Hockenhull, K., Wickham, H., Harman, S., and Armstrong, L.: High-frequency water quality time series in precipitation and streamflow: From fragmentary signals to scientific challenge, Sci. Total Environ., 434, 3–12, https://doi.org/10.1016/j.scitotenv.2011.10.072, 2012.

Pasari, S.: A review of empirical orthogonal function (EOF) with an emphasis on the co-seismic crustal deformation analysis, Nat. Hazards, 110, 29–56, https://doi.org/10.1007/s11069-021-04967-4, 2022.

Preisendorfer, R. W. and Mobley, C. D.: Principal component analysis in meteorology and oceanography, Elsevier, Amsterdam Oxford New York [etc.], 1988.

R Core Team: _R: A Language and Environment for Statistical Computing_, 2023.

Rode, M. and Suhr, U.: Uncertainties in selected river water quality data, Hydrol. Earth Syst. Sci., 11, 863–874, https://doi.org/10.5194/hess-11-863-2007, 2007.

Rode, M., Arhonditsis, G., Balin, D., Kebede, T., Krysanova, V., Van Griensven, A., and Van Der Zee, S. E. A. T. M.: New challenges in integrated water quality modelling, Hydrol. Process., 24, 3447–3461, https://doi.org/10.1002/hyp.7766, 2010.

Rode, M., Halbedel Née Angelstein, S., Anis, M. R., Borchardt, D., and Weitere, M.: Continuous In-Stream Assimilatory Nitrate Uptake from High-Frequency Sensor Measurements, Environ. Sci. Technol., 50, 5685–5694, https://doi.org/10.1021/acs.est.6b00943, 2016.

Sabater, S., Artigas, J., Durán, C., Pardos, M., Romaní, A. M., Tornés, E., and Ylla, I.: Longitudinal development of chlorophyll and phytoplankton assemblages in a regulated large river (the Ebro River), Sci. Total Environ., 404, 196–206, https://doi.org/10.1016/j.scitotenv.2008.06.013, 2008.

Schröter, D., Zebisch, M., and Grothmann, T.: Climate change in Germany. Vulnerability and Adaptation of Climate Sensitive Sectores, Deutscher Wetterdienst, 2005.

Seibertz, E.: Das Hilskonglomerat in der Unterkreide-zeitlichen Braunschweiger Bucht - Teil I: Die bioklastische Fazies des Hilskonglomerates als kartierbare Einheit und Klimazeuge, Braunschweiger Naturkundliche Schriften, 16Braunschweiger Naturkundliche Schriften, 83, https://doi.org/10.24355/DBBS.084-202011251541-0, 2020.

Shrestha, S. and Kazama, F.: Assessment of surface water quality using multivariate statistical techniques: A case study of the Fuji river basin, Japan, Environ. Model. Softw., 22, 464–475, https://doi.org/10.1016/j.envsoft.2006.02.001, 2007.

United Nations Environment Programme: Water Quality for Ecosystem and Human Health: Second Edition, UN Environment Document Repository, 2008.

Walling, D., Webb, B., and Woodward, J.: Some sampling considerations in the design of effective strategies for monitoring sediment-associated transport, in: Erosion and sediment monitoring programmes in river basins. Proc. international symposium, Oslo, 1992|, vol. 210, International Association of Hydrological Sciences, 279--288, 1992.

Weyer, C., Peiffer, S., Schulze, K., Borken, W., and Lischeid, G.: Catchments as heterogeneous and multi-species reactors: An integral approach for identifying biogeochemical hot-spots at the catchment scale, J. Hydrol., 519, 1560–1571, https://doi.org/10.1016/j.jhydrol.2014.09.005, 2014.

https://doi.org/10.5194/egusphere-2026-1203
Preprint. Discussion started: 9 April 2026

Winter, C., Lutz, S. R., Musolff, A., Kumar, R., Weber, M., and Fleckenstein, J. H.: Disentangling the Impact of Catchment Heterogeneity on Nitrate Export Dynamics From Event to Long-Term Time Scales, Water Resour. Res., 57, e2020WR027992, https://doi.org/10.1029/2020WR027992, 2021.

Wollschläger, U., Attinger, S., Borchardt, D., Brauns, M., Cuntz, M., Dietrich, P., Fleckenstein, J. H., Friese, K., Friesen, J., Harpke, A., Hildebrandt, A., Jäckel, G., Kamjunke, N., Knöller, K., Kögler, S., Kolditz, O., Krieg, R., Kumar, R., Lausch, A., Liess, M., Marx, A., Merz, R., Mueller, C., Musolff, A., Norf, H., Oswald, S. E., Rebmann, C., Reinstorf, F., Rode, M., Rink, K., Rinke, K., Samaniego, L., Vieweg, M., Vogel, H.-J., Weitere, M., Werban, U., Zink, M., and Zacharias, S.: The Bode hydrological observatory: a platform for integrated, interdisciplinary hydro-ecological research within the TERENO Harz/Central German Lowland Observatory, Environ. Earth Sci., 76, 29, https://doi.org/10.1007/s12665-016-6327-5, 2017.

Yue, F.-J., Li, S.-L., Waldron, S., Oliver, D. M., Chen, X., Li, P., Peng, T., and Liu, C.-Q.: Source availability and hydrological connectivity determined nitrate-discharge relationships during rainfall events in karst catchment as revealed by high-frequency nitrate sensing, Water Res., 231, 119616, https://doi.org/10.1016/j.watres.2023.119616, 2023.

Yue, W., Meng, K., Hou, K., Zuo, R., Zhang, B.-T., and Wang, G.: Evaluating climate and irrigation effects on spatiotemporal variabilities of regional groundwater in an arid area using EOFs, Sci. Total Environ., 709, 136147, https://doi.org/10.1016/j.scitotenv.2019.136147, 2020.

Zacharias, S., Bogena, H., Samaniego, L., Mauder, M., Fuß, R., Pütz, T., Frenzel, M., Schwank, M., Baessler, C., Butterbach-Bahl, K., Bens, O., Borg, E., Brauer, A., Dietrich, P., Hajnsek, I., Helle, G., Kiese, R., Kunstmann, H., Klotz, S., Munch, J. C., Papen, H., Priesack, E., Schmid, H. P., Steinbrecher, R., Rosenbaum, U., Teutsch, G., and Vereecken, H.: A Network of Terrestrial Environmental Observatories in Germany, Vadose Zone J., 10, 955–973, https://doi.org/10.2136/vzj2010.0139, 2011.

Zhang, X., Yang, X., Jomaa, S., and Rode, M.: Analyzing impacts of seasonality and landscape gradient on event-scale nitrate-discharge dynamics based on nested high-frequency monitoring, J. Hydrol., 591, 125585, https://doi.org/10.1016/j.jhydrol.2020.125585, 2020.

Zhang, X., Yang, X., Hensley, R., Lorke, A., and Rode, M.: Disentangling In-Stream Nitrate Uptake Pathways Based on Two-Station High-Frequency Monitoring in High-Order Streams, Water Resour. Res., 59, e2022WR032329, https://doi.org/10.1029/2022WR032329, 2023.

Zink, M., Kumar, R., Cuntz, M., and Samaniego, L.: A high-resolution dataset of water fluxes and states for Germany accounting for parametric uncertainty, Hydrol. Earth Syst. Sci., 21, 1769–1790, https://doi.org/10.5194/hess-21-1769-2017, 2017.